

**Swiss Federal Office of Energy SFOE** Section Energy Research and Cleantech

Rapport final du 20 Décembre 2018

# Combined service station for battery electric & hydrogen fuel cell vehicles



© EPFL 2016





Laboratoire d'électrochimie







Date: 20 Décembre 2018

Lieu: Martigny

#### Prestataire de subventions :

Confédération suisse, représentée par L'Office fédéral de l'énergie OFEN Programme pilote, de démonstration et Programme-phare CH-3003 Berne www.ofen.admin.ch

#### Bénéficiaires de la subvention :

**EPFL-LEPA EPFL Valais Wallis** Rue de L'Industrie 17, CP 440 CH-1951 Sion www.lepa.epfl.ch

Sinergy SA Rue du Simplon 4b CH-1920 Martigny www.sinergy.ch

Centre de Recherches Energétiques et Municipales (CREM) Rue du Grand-Saint-Bernard 4 CH-1920 Martigny www.crem.ch

Ville de Martigny Rue des Ecoles 1 CH-1920 Martigny www.martigny.ch

#### Auteurs:

Yorick Ligen, EPFL Valais Wallis - LEPA, yorick.ligen@epfl.ch Hubert Girault, EPFL Valais Wallis - LEPA, hubert.girault@epfl.ch Jakob Rager, CREM, jakob.rager@crem.ch

Direction du programme de l'OFEN : Yasmine Calisesi, yasmine.calisesi@bfe.admin.ch Suivi du projet pour l'OFEN : Stefan Oberholzer, stefan.oberholzer@bfe.admin.ch

Numéro du contrat de l'OFEN : SI/501286-01

Les auteurs sont seuls responsables du contenu et des conclusions de ce rapport.

#### Office fédéral de l'énergie OFEN

Mühlestrasse 4, 3063 Ittigen, Adresse postale: 3003 Berne Tél. +41 58 462 56 11 · fax +41 58 463 25 00 · contact@bfe.admin.ch · www.ofen.admin.ch



## Zusammenfassung

Das Projekt «Kombinierte Tankstelle für batterieelektrische Autos und /oder Wasserstofffahrzeuge» startete am 1. Dezember 2015 und wurde am 30. November 2018 abgeschlosssen. Dieser Abschlussbericht beschreibt de Resultate über das gesamte Projekt. Das Projekt ist unterteilt in die folgenden Arbeitspakete: Technische Installation und Vorbereitung der Anlage (WP1), Hardware Installation (WP2), Automatisierung und Programmierung des Steuersystems (WP3), Messkampagne und Auswertung des Systems (WP4), Technische Studien und Modelierung (WP5), Kommunikation und Wissentransfer (WP6).

In WP1 und WP2, wurde eine Ladestation installiert, die mit einer Vanadium RedoxFlow Batterie (VRFB) gekoppelt ist. Dazu wurde auch eine Wasserstofftankstelle mit vor Ort Elektrolyse errichtet. Die Tankstelle ist seit September 2016 in Betrieb. Das Design ermöglicht eine hohe Einsatzflexibilität. Verschiedene Fahrzeuge wie ein Swiss Hydrogen Kangoo (1.5 kg bei 350 bar), ein Hyundai ix35 Fuel Cell (5 kg bei 700 bar) und des Green GT H2 (8 kg bei 700 bar) haben an dem Demonstrator getankt.

In WP3, wurde das Kontrollsystem und die Datenerfassung programmiert und implementiert. Unter nominalen Betriebsbedigungen, können 0.75 kg H<sub>2</sub> pro Stunde bei 200 bar produzierte, gereignigt und gelagert werden.

In WP4, dank der Entwicklung von spezifischer Hardware und Software, haben wir zahlreiche Daten gesammelt. Während des Betriebs der Wasserstofftankstelle werden 28 Variablen und für den Elektrolyseur 43 Variablen pro Sekunde aufgezeichnet. Dies ermöglicht eine genaue Prozessmodellierung und Identifizierung von Energieverlusten.

In WP5 und WP6, haben wir zahlreiche Kontakte und Erfahrungsaustausch mit privaten Unternehmen (Green GT, H55, Enerox), Versorgungsunternehmen (ESR, SIG), akademischen Partnern (HES-SO Valais Wallis, Swiss Competence Center for Energy Research – Heat and Electricity storage (SCCER-HaE), University of Strathclyde) und der Öffentlichkeit (Rallye du Valais, Swiss Mobility Days, verschiedene Interviews und Berichterstattung mit RTS, Le Nouvelliste, Le Temps, Le Matin) aufgebaut. Es wurden 3 wissenschaftliche Arbeiten veröffentlicht, zwei weitere befinden sich in der Endphase der Redaktion und zwei weitere werden nach zusätzlicher Datenerhebung erwartet.



## Résumé

Le projet « Station-service combinée pour voitures électriques avec batteries et / ou piles à combustible » a débuté le 1<sup>er</sup> Décembre 2015 et s'est achevé le 30 Novembre 2018. Ce rapport final décrit les résultats obtenus sur l'ensemble du projet. Le projet est divisé en six blocs de travail: Achats et travaux préliminaires d'aménagement (WP1), Installation des systèmes électrochimiques et des bornes de recharge (WP2), Mise en place du système de contrôle (WP3), Etudes, mesures et évaluation du système (WP4), Etude technico-économique (WP5), Démonstration, transfert de connaissance et communication (WP6).

Les WP1 et WP2 ont permis l'installation d'une borne de recharge électrique couplée avec une batterie redox à flux au Vanadium (VRFB) et la construction d'une station de recharge hydrogène avec production sur site. La station a été inaugurée en septembre 2016 et est en opération depuis lors. Le design offre une grande flexibilité pour permettre le remplissage de véhicules variés tels que la Kangoo modifiée par Swiss Hydrogen (1.5 kg à 350 bar), la Hyundai ix35 Fuel Cell (5 kg à 700 bar) et la Green GT H2 Speed (8 kg à 700 bar).

Dans le WP3, le système de contrôle ainsi que les protocoles de communication entre tous les soussystèmes ont été programmés et implémentés pour un fonctionnement synchronisé du démonstrateur. Dans les conditions nominales, 0.75 kg d'hydrogène par heure peuvent être produits, purifiés et stockés à 200 bar.

Au cours des campagnes de mesure du WP4, nous avons pu tirer pleinement parti des systèmes construits et programmés par nos soins dans les WP1, WP2 et WP3. Chaque seconde, 28 variables sont enregistrées durant le fonctionnement de la station de remplissage d'hydrogène, et 43 variables pendant le fonctionnement de l'électrolyseur. Ces données permettent de modéliser précisément les processus et d'identifier les pertes énergétiques.

Enfin les WP5 et WP6, ont généré beaucoup d'intérêt et permis d'échanger savoir-faire et connaissances avec des entreprises privées (Green GT, H55, Enerox), des services industriels (ESR, SIG), des partenaires académiques (HES-SO Valais Wallis, Swiss Competence Center for Energy Research – Heat and Electricity storage (SCCER-HaE), University of Strathclyde) et le public dans son ensemble (Rallye du Valais, Swiss Mobility Days, diverses interviews et reportages sur la RTS, Le Nouvelliste, Le Temps, Le Matin). 3 articles scientifiques ont été publiés, 2 en sont à l'étape finale de rédaction et deux supplémentaires sont attendus après d'autres campagnes de mesures.



## **Abstract**

The project entitled "Combined service station for battery electric cars and hydrogen fuel cell vehicles" started on the 1<sup>st</sup> of December 2015 and was finished on the 30<sup>th</sup> of November 2018. The results obtained during this period are reported here. The project was divided into six work packages: Technical installation and preparation of the building (WP1), Hardware installation (WP2), Automation and programming of the control system (WP3), Measurements and data analysis (WP4), Technical studies and modelling (WP5), Communication and knowledge transfer (WP6).

In WP1 and WP2, an electric charging station coupled with a vanadium redox flow battery (VRFB) was installed and a hydrogen refilling station with on-site hydrogen production was built. The fueling station was inaugurated in September 2016 and is in operation since then. The design allows a high flexibility to refill various vehicles such as a Swiss Hydrogen Kangoo (1.5 kg at 350 bar), a Hyundai ix35 Fuel Cell (5 kg at 700bar) and the Green GT H2 Speed (8 kg at 700 bar).

In WP3, the control software and communication protocols between all subsystems were programmed and implemented for a synchronized operation of the demonstrator. In nominal operating conditions, 0.75 kg of H<sub>2</sub> per hour can be produced, purified and stored at 200 bar.

In WP4, the whole benefits of the custom hardware and software realized in WP1, WP2 and WP3 were fully exploited for measurements. 28 variables are recorded every second during the operation of the refilling station and 43 variables per second for the electrolyser allowing an accurate process modelling and identification of energy losses.

In WP5 and WP6, we successfully generated interest and shared knowledge with private companies (Green GT, H55, Enerox), public utilities (ESR, SIG), academic partners (HES-SO Valais Wallis, Swiss Competence Center for Energy Research – Heat and Electricity storage (SCCER-HaE), University of Strathclyde) and the general public (Rallye du Valais, Swiss Mobility Days, various interviews and coverage with RTS, Le Nouvelliste, Le Temps, Le Matin). 3 scientific papers were published, another 2 are in the final stage of redaction and two more are expected after additional data collection.



## Take-home messages

- Using large scale commercially available equipments, energy losses in the range of 34 to 43% are occurring on the "Intermittent grid to vehicle" charging infrastructure for battery electric and hydrogen fuel cell vehicles
- The overall energy efficiency of the installed vanadium redox flow battery was measured at a maximum of 60%. The energy efficiency is heavily impacted by power electronics (up to 24% of losses) and a non-optimized battery management system
- The opportunity to use mega batteries for grid stability, renewable integration and auto consumption of industrial sites appears to be limited. However, a local energy storage system of 600 kWh/300 kW can reduce the grid connection for a 6-stalls fast charging station (up to 1000 charging events per week) from 900 kW to 600 kW.
- Successful operation of a 20 kg/day hydrogen refueling station with on-site electrolysis, designed, engineered and built in-house. Various refueling modes for 350 and 700 bar vehicles are possible by a highly versatile system. More than 60 variables are monitored along the grid to mobility conversion processes.



## **Sommaire**

Zusammenfassung	3
Résumé	4
Abstract	5
Take-home messages	6
Sommaire	7
Introduction and background	9
Motivation of the project and goals Project overview	
Redox flow battery operation	11
Operation and characterization Technical Hurdles	
Energy storage systems integration	14
Integration in Martigny's MV grid	14
Self-consumption and self-sufficiency with PVs and batteries	
Sizing and operation in the context of a charging station	16
Results	17
Electrolysis systems	
Design and control strategies  AC/DC and DC/DC considerations  Design	19
Control system	
Purification and storage Measurements and performance	
Hydrogen compression and filling	28
Compression system	
Hydrogen refueling station	30
Conclusions and outlook	33
Acknowledgments	34
Publications and outreach	34
Journal papers	34



International conferences	35
In the press and various events	35
Références	36
Annexes	37
Supplier specifications of main equipments	37
Alkaline Electrolyser: McPhy, McLyzer 10-10	37
PEM Stack: Giner, Merrimack 14 cells, 900 A	38
Gas booster: Maximator, DLE-5, DLE-15-2, DLE-30-2, DLE-75-2	39
Redox Flow Battery: Gildemeister, FB 200-400	40
Electrical Charger: EVTec espresso&charge	41
DC/DC converter for electrical charger: Brusa, BDC546-B06 (bidirectional)	42
Air compressor: Kaeser, BSD 75 SFC	43
List of component suppliers	44
Sensors	44
Control valves	44
Pumps	44
Others	44
Open Access publications	45
World Electric Vehicle Journal	45
Batteries	45
Lista das abráviations	45



## Introduction and background

## Motivation of the project and goals

Electric and hydrogen mobility are recognised as a necessary step within the energy transition. The transport related emissions and efficiency losses are thus shifted from the vehicles to the infrastructure and the supply chain of the energy carrier. A specific attention should therefore be paid to the deployment and integration of hydrogen refilling stations (HRS) and electric charging stations.

Regarding hydrogen mobility, Japan, Germany, and California are leading the way with respectively 100, 53 and 35 HRS in operation in late 2018<sup>1</sup>. Most of these stations are designed for 200 to 400 kg of H<sub>2</sub> dispensed per day, but due to the limited number of vehicles, the average amount dispensed is equal to 5 kg/day in Japan, 4 kg/day in Germany and 40 kg/day in California. In addition, despite the advantages of on-site electrolysis, most of the stations receive hydrogen *via* tube trailers and a large share of the hydrogen comes from steam reforming of natural gas.

On the other side, the network of electric chargers is growing rapidly with more than 400 Tesla supercharging stations in Europe<sup>2</sup> (17 in Switzerland) and even more with the CCS and CHAdeMO plugs. The largest stations have more than 20 charging points per site, representing a peak load on the grid exceeding 2 MW, without a correlation with local renewable electricity availability.

For a better integration of electric charging stations and hydrogen filling stations within the energy system, LEPA had proposed to develop a combined service station. The goal was to investigate the appropriate sizing and to measure the efficiency of each steps along the way from grid to mobility. Together with the City of Martigny, Sinergy and CREM, the "Combined service station" project was launched to demonstrate the feasibility of such a system, develop the local know-how and engage discussions in political and public exchanges. As a preliminary work, an overall energy efficiency assessment was realized to compare the different pathways from grid to mobility [1] (available in Appendix 0).

## **Project overview**

All the components installed for the project are presented in **Figure 1**. The demonstrator is organized around three main electrochemical devices: a 200 kW/400 kWh vanadium redox flow battery (VFRB) analyzed in section 0 and two electrolysis systems studied in section 0. The high-pressure hydrogen processing and dispensing unit are described in section 0. Eight programmable logic controllers (PLC) are used to control the different subsystems, and all the data are logged and analyzed in a dedicated control room.

<sup>&</sup>lt;sup>1</sup> https://www.energy.gov/sites/prod/files/2018/10/f56/fcto-infrastructure-workshop-2018-16-ikeda.pdf, https://h2.live/, https://cafcp.org/stationmap

https://www.electrive.com/2018/06/28/europe-tesla-supercharger-network-at-3200-charge-points/



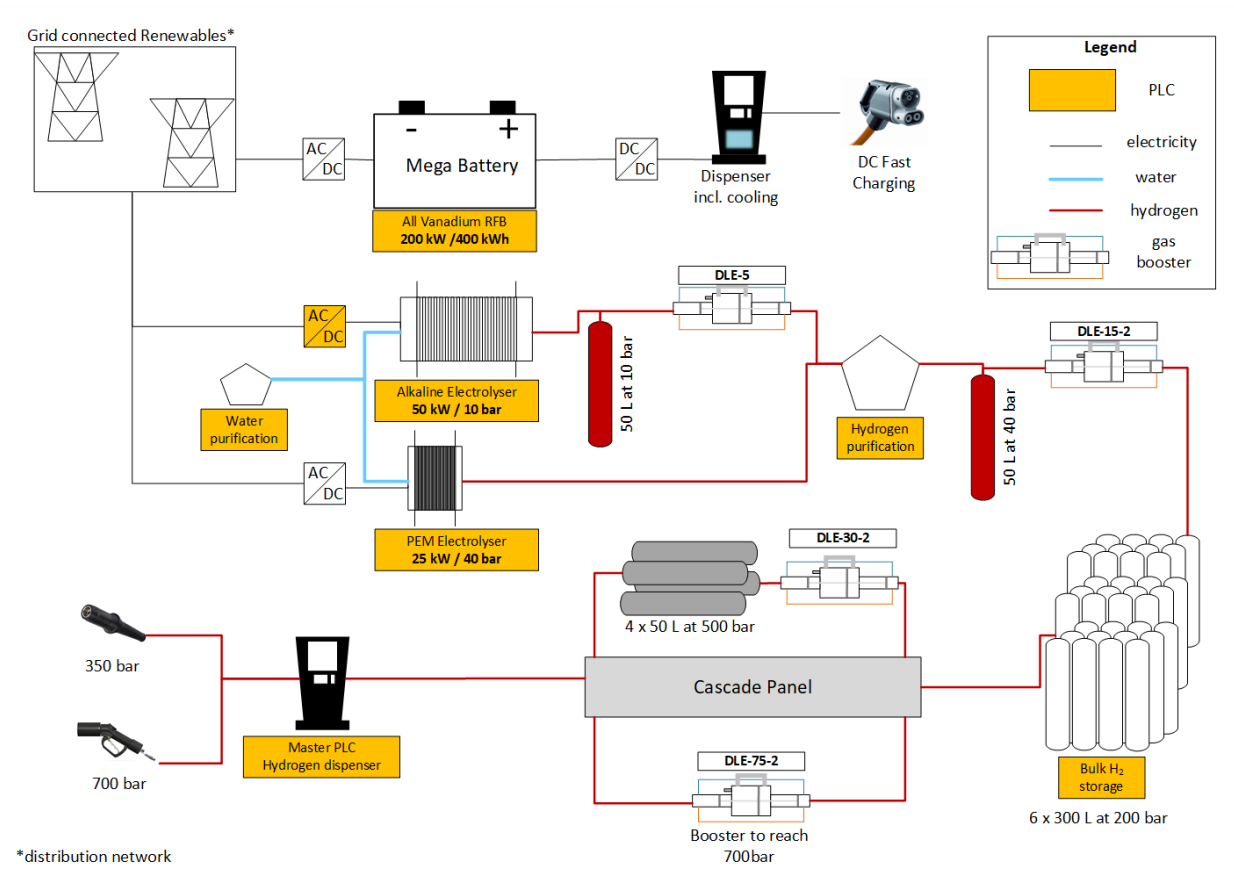


**Figure 1** - Overview of the systems installed in the demonstrator and corresponding controllers (for readability purposes, the air compressor, which feeds the gas boosters is not represented)



## **Redox flow battery operation**

## Operation and characterization

This subsection is fully covered in Appendix 0 [2].





Figure 2 - Aerial view of the 200 kW/ 400 kWh VRFB, and inside view of the upper container with the stacks

#### **Technical Hurdles**

The LEPA operates demonstrator scale vanadium redox flow batteries (VRFBs) since 2013, when a dual flow circuit project supported by the SFOE started in Martigny [3]. Despite marginal differences in stack dimensions, the 200 kW / 400 kWh studied here and the 10 kW / 40 kWh studied in 2013 present similar materials and design (GildeMeister, Austria). Thanks to the expertise developed with the operation of both systems, we have recognised some similar degradation processes. Indeed, both batteries failed (evidenced by leakages from the stacks) and exhibited same symptoms in the post-mortem analysis: corrosion of the carbon electrodes on the positive side. It is known that when a cell is overcharged, possible side reactions, such as hydrogen evolution, can occur at the cathode. This gas evolution affects the flow of the electrolyte, creates imbalance, increases the cell resistance and alters the pH of the solution [2]. Two scenarios can be proposed for the corrosion rate of the electrode.

Scenario A: The imbalance of the electrolyte, linked to side reactions such as hydrogen evolution, leads to an improper measurement of the state of charge of the battery. The overcharging potential can thus trigger electrode corrosion.

Scenario B: Shunt currents and the heterogeneous conductivity of the bipolar plates may create hot spots and degrade the electrode with a feedback loop.

In both cases, the development of a new battery management system (BMS) should help to prevent this type of failure. This topic is currently being discussed with the company which took over the original supplier.

In **Figure 3**, a leakage resulting from the dissolution of the current collector was observed, and the disassembly of the stack confirmed the diagnosis.





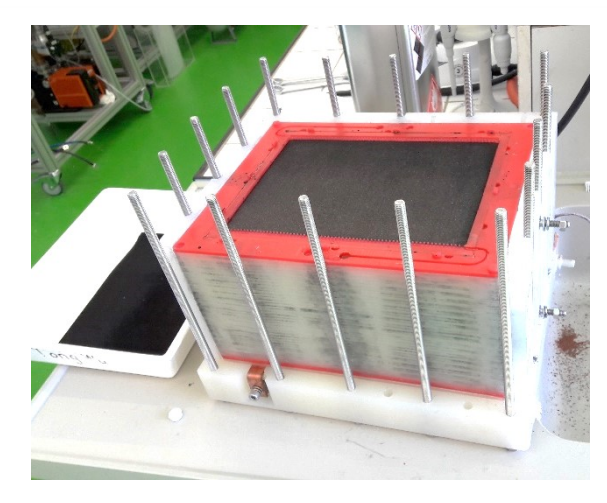
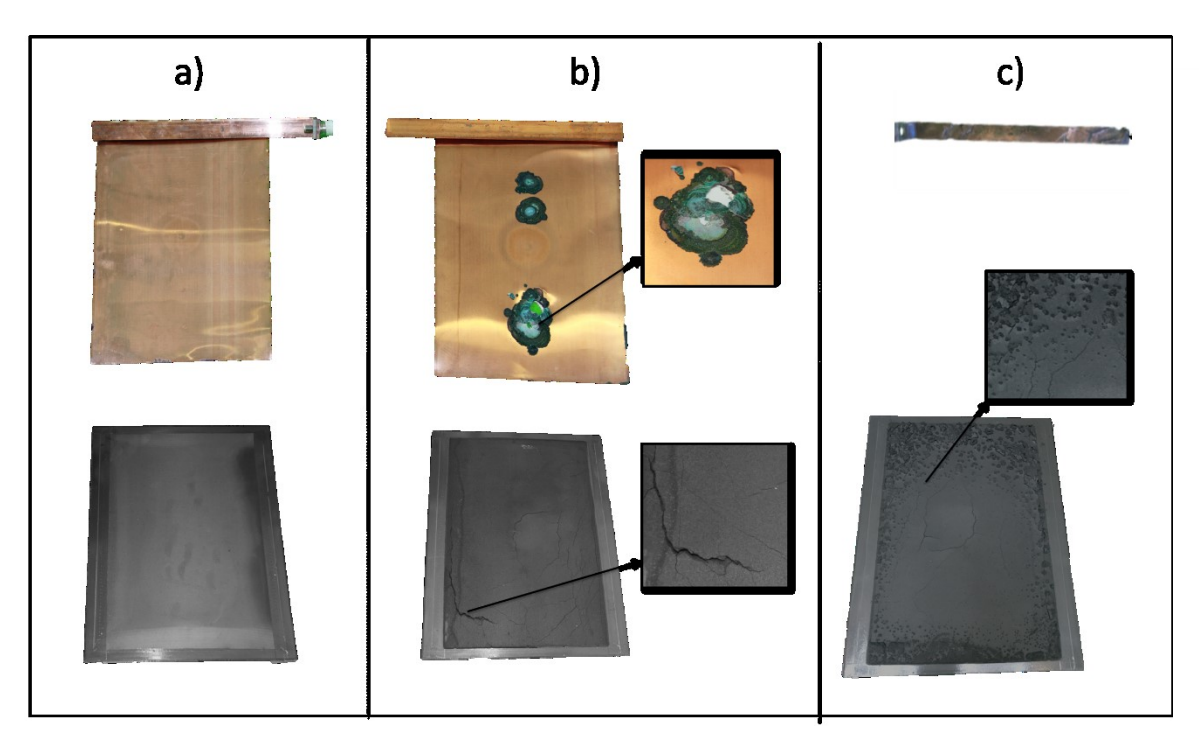


Figure 3 - Leakage of electrolyte in the system and stack disassembly in the lab

In **Figure 4**, several stacks from the 10 kW / 40 kWh battery were disassembled. We observed that the presence of cracks on the last bipolar plate allowed the contact between the positive electrolyte and the copper current collector. Subsequently, the dissolution of copper progressed until the total failure of the stack. More important, it was found that the copper has a catalytic effect on hydrogen evolution, and thus the imbalance of the electrolyte, leading to a negative feedback loop. Therefore, a procedure to purify the electrolyte after such stack failure was specifically developed during the project. A pilot installation was built, and we successfully recovered the electrolyte from the 10 kW / 40 kWh system.





**Figure 4** - Pictures of copper current collector and bipolar plate of a VRFB stack: (a) No corrosion (b) Marked corrosion (c) Advanced corrosion.

Several warranty repairs were organised for the 200 kW / 400 kWh system. From the beginning, high levels of hydrogen inside of the electrolyte tank were measured. After discovering the dissolution of several copper current collectors, an intervention for trying to clean the electrolyte was carried out by the service team of the original supplier in December 2016. In March 2017, the attempt was declared unsuccessful, and a full replacement of the 27 m³ of electrolyte and a replacement of 40 stacks was organized. The battery was put back in operation in April 2017. However, the implemented measures to avoid further degradation of the system were insufficient and hydrogen was still produced in the electrolyte tanks. The original supplier company filed for bankruptcy in October 2017, and we had to wait until July 2018 to initiate new discussions with the new owner, Enerox (Austria).

Based on these investigations and issues, it was decided to replace the existing stacks with alternative designs. For the 10 kW / 40 kWh, seal free stacks designed by Volterion³ (Germany) are being installed. And for the 200 kW / 400 kWh, the next generation of stacks developed by Enerox (Austria) should be installed in Spring 2019. The stack design was specifically improved to avoid the dissolution of copper, and a specific attention will be paid to the BMS.

<sup>&</sup>lt;sup>3</sup> https://www.volterion.com/en/stack-en/



## **Energy storage systems integration**

This section was to a large extent covered by the work of the CREM, using data from Sinergy in order to address the questions of WP5. The first subsection covers the integration of energy storage systems (ESS) in the medium voltage (MV) grid of Martigny, the second one covers the use of ESS in the case of small and medium businesses, and finally the integration in BEV charging stations was specifically modelled by EPFL and will be subject to a publication.

## Integration in Martigny's MV grid

The first step of our work was to investigate whether or not the installation of a storage unit could improve the grid's operational management in Martigny's MV grid in the case of massive development of new renewable energy (NRE) and new loads. Battery capacities and powers needed for this purpose were also investigated.

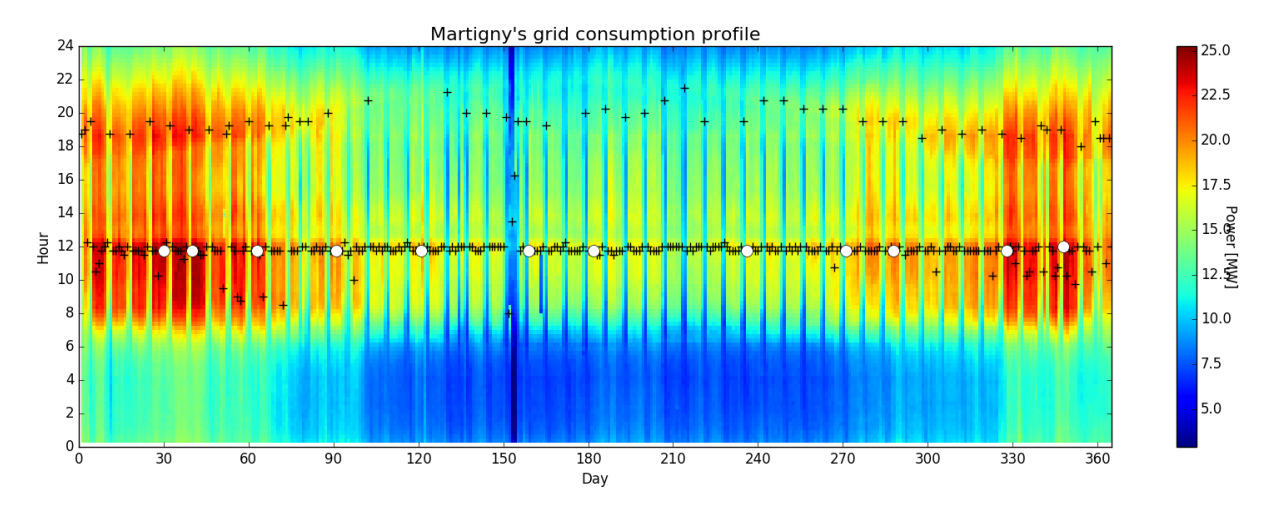


**Figure 5** - The consumption profile in Martigny's MV grid for year 2015. Black "+" signs represent maximum power demand within a day and white "o" signs maximum power demand within each month.

#### Methodology

Data provided by Synergy, the local utility, were collected for simulation purposes. It encompasses:

- MV grid topology and associated lines parameters
- Consumption and production data with a 15 minutes step

Data were processed and simulations performed in order to obtain voltages, currents and power losses evolutions for different scenarios using a Newton Raphson algorithm. We decided to simulate only the longest line of Martigny's grid where a photovoltaic power station and a wind turbine are installed. In fact, it appeared to be the line with the highest probability for a storage unit installation improving the management of the grid.



The different scenarios for grid simulations were:

- Current state MV grid,
- MV Grid with a large load added,
- MV Grid with a large photovoltaic power station added
- MV Grid with a large photovoltaic power station and a battery (different capacities and powers) added,

High-level of interconnections within branches of Martigny's grid and with adjacent MV grids makes standalone grid operation scenario not relevant. Therefore, this scenario will not be analysed for this MV grid operations management study.

#### Results

Results show that in its current state, the MV Martigny's grid has been designed with sufficient robustness to support any usual operation. Voltage deviations are around 1% the nominal voltage (16 kV) and peak currents are around one third the admissible value (200 A). Currents have been shown to be more limiting than voltage deviations. As being a small and urban grid, lines lengths are rather short leading to small impedances and small voltage deviations.

In order to test grid robustness, large loads and PV farms have been added at the end of the longest branch. With a load consuming twice the global branch consumption, voltages and currents stays in an admissible range. In contrast, with a 4 MW PV power station and coupled with the existing wind turbine, currents overpass the admissible range during sunny and windy summer days. In this case, grid operators would have to reinforce certain lines.

Alternatively, a battery could be added in order to shave power peak production. Simulations show that the battery size should be around 5 MW/2.5 MWh (a lot larger than the 200 kW/400 kWh battery used in this project) in order to have an effective impact (reduce peak current from 200 A to 160 A). However, the battery will only be really useful during peak production in summer, whereas in winter, currents will always stay under admissible range.

Moreover, the investment in a battery of such a size amounts to several million CHF, while grid reinforcement investment (Network infrastructure) will hardly overpass a few hundreds of thousands CHF. Finally, when a failure occurs, the number of coupling stations is large enough to insure power delivery in the whole grid without really perturbing grid operations.

In conclusion, even with quite unrealistic development scenarios such as large loads and PV installations, Martigny's grid will hardly lead to a case where its reinforcement is needed. Therefore, from a technical point of view, installing batteries is not suitable considering the current state of the MV grid and current battery prices. We conclude that the required battery size represents currently a very uneconomical solution.



## Self-consumption and self-sufficiency with PVs and batteries

Using consumption data from a set of local small and medium enterprises (SMEs), we investigated the relevance of stationary batteries in order to increase self-consumption and self-sufficiency from a local PV production. A large variety of profiles was studied with 5, 6 and 7 days of operation per week. For data privacy reasons, the report cannot be publicly reproduced here.

A battery control algorithm maximizing the self-sufficiency was developed and the simulation with both solar and consumption data was realized over one full year.

The main findings are that the batteries do indeed increase both the self-sufficiency and the self-consumption (from 5% to 50%) but their amortization times are not acceptable for SMEs with the current electricity pricing scheme and battery costs. However, batteries are found to be underused (30% - 95% down times). If this effect is taken into account, it might be possible to aggregate other grid services and to reach amortization times below 10 years.

## Sizing and operation in the context of a charging station

The availability of medium voltage connection limits the deployment of 150 kW chargers in multistall service stations. In addition, the power consumption profile of such stations results in high cost penalties due to monthly power peaks (6 CHF/kW/month with Sinergy) and linkage fees (up to 100 CHF/kW). The installation of an ESS at the station can address these two issues.

#### Methodology

As limited data is available for the usage of fast charging stations, a stochastic distribution of charging events was used to model power demand profiles. We assumed 20 min charging sessions with a maximum power of 150 kW. An algorithm considering the number of charging events per week and the maximum contracted power for the grid connection was implemented. This algorithm returns the required battery capacity, the power demand profile at the station and the power delivered by the grid with a resolution of one minute. Frequentations in the range of 25 to 2000 vehicles per week, and grid connections ranging from 25 kW to 3 MW were investigated.



#### **Results**

Without ESS, a MW range connection to the grid is necessary for charging stations with more than 6 charging points. However, this maximum grid connection is needed for only a few peak events per week as presented in **Figure 6**.

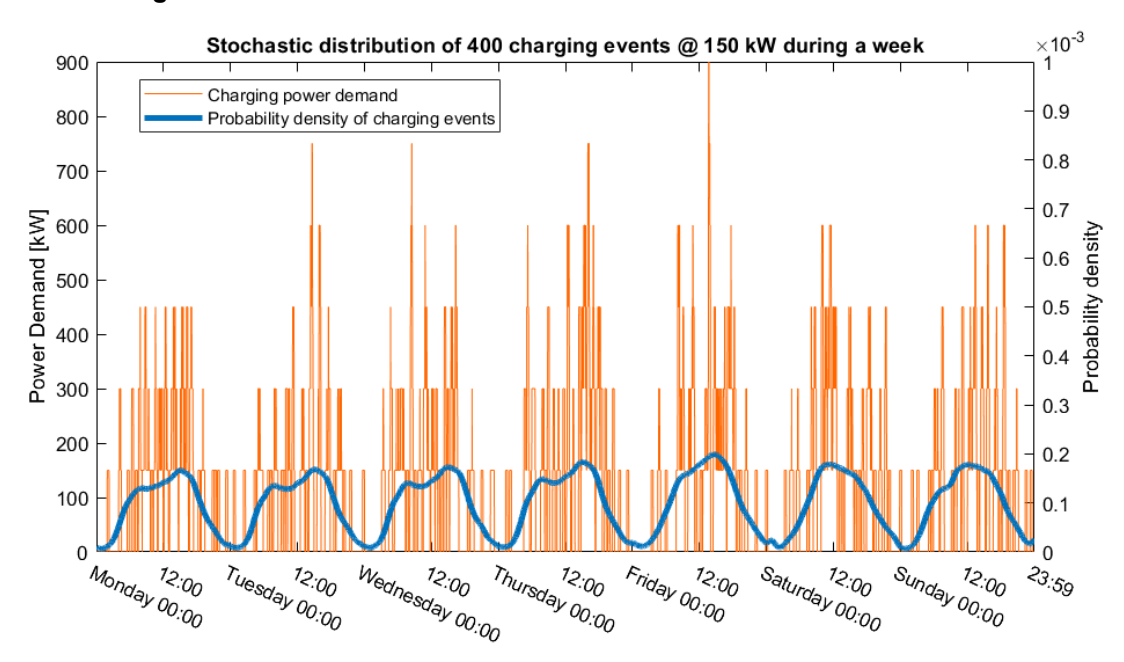


Figure 6 - Power profile for a charging station with 400 charging events per week, based on stochastic distribution

We demonstrate that a 500 kW grid connection and a 1 MWh battery is sufficient in all scenarios with up to 8 charging points. And for smaller stations, a 300 kWh/600kW battery associated with a 300 kW grid connection should fulfill most of the cases in the Swiss context. An exemplary week with 6 charging points and 400 charging events is presented in **Figure 7**. The battery is discharged only when the charging demand exceeds the grid connection, and thus the 300 kWh/600kW system reduce the peak power demand from the grid by a factor 3. Thus, demand side management techniques are not required and the customer experience is maintained even during peak hours. Considering a power fee of 6 CHF/kW/month<sup>4</sup>, more than 40 kCHF can be saved annually, with minor efficiency losses.

A queuing system was also implemented in the algorithm to find the optimum number of charging points, ensuring that a limited share of the users will wait more than 5 minutes at the station.

-

<sup>4</sup> https://sinergy.ch/tarifs/ 2018



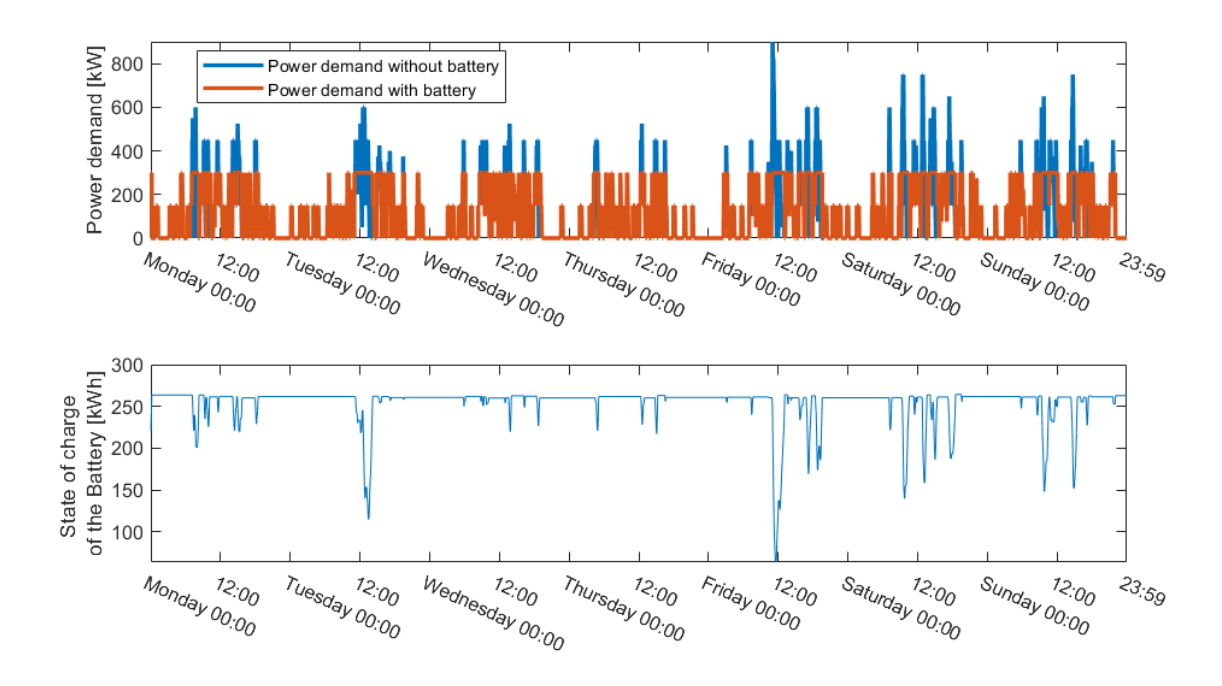


**Figure 7** - Peak power reduction with a local 300 kWh/600 kW energy storage system. 400 charging events per week at 150 kW.



## **Electrolysis systems**

## Design and control strategies

#### AC/DC and DC/DC considerations

In the proposal, a DC connection between the VRFB and the electrolyser was proposed. However, several technical issues did not allow this innovation to be implemented. Indeed, the availability of off-the-shelf DC/DC converters, for the wide range of current and voltage required (see **Table 1**), was a major hurdle. Also, the VRFB has a ground isolated DC bus architecture while the negative pole of the electrolyser is grounded.

	DC Bus VRFB	DC Charger	Alkaline Electro- lyser (per stack)	PEM Electro- lyser
Voltage	700 V	500 V	250 V	30 V
Current	30 - 280 A	160 A	60 - 115 A	90 – 900 A

Table 1 - DC/DC Power Electronics requirements

Moreover, the issues detailed in subsection 0 and efficiency considerations, lead us to keep electrolysis and VRFB systems decoupled in order to ensure independent operations. An adequate power metering was installed in order to differentiate AC/DC losses from the rest of the system. The alkaline electrolyser is operated with the original AC/DC converter delivered by the supplier, and the PEM electrolyser is mounted with an AC/DC converter from Magna Power (USA). Their respective efficiencies are 92-95% (measured) and 86% (based on supplier specifications). The high current, up to 900 A, required for the PEM inevitably leads to higher transformation losses, and requires an additional active cooling system for the power supply. We can note that the AC/DC converter of the VRFB has a measured efficiency of 96-97% (see section 0).

#### Design

The PEM electrolyser was built around a 25 kW stack from Giner (USA), while the alkaline electrolyser was reengineered and rebuilt around a 50 kW system from McPhy (France). The technical drawings are presented in **Figure 9** and **Figure 8**. A water purification system (reverse osmosis, and ion-exchange column) has been installed upstream.

The initial project sketch was to buy ready to plug commercial equipments but due to multiple failures and misconceptions on both hardware and software levels of the McPhy electrolyser, we decided to reengineer the alkaline system and to build our own PEM system. This decision was difficult to take, but greatly improved the system control and data logging possibilities.



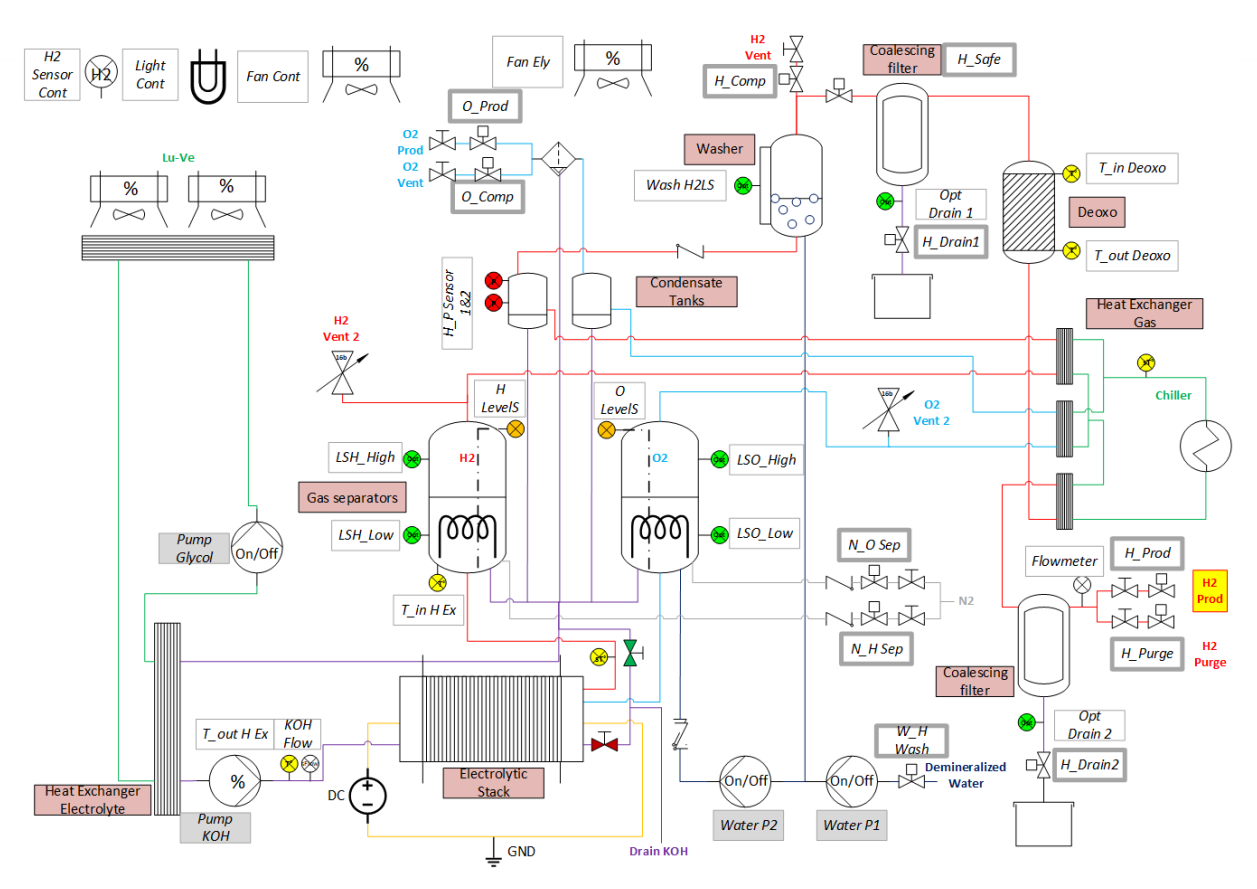
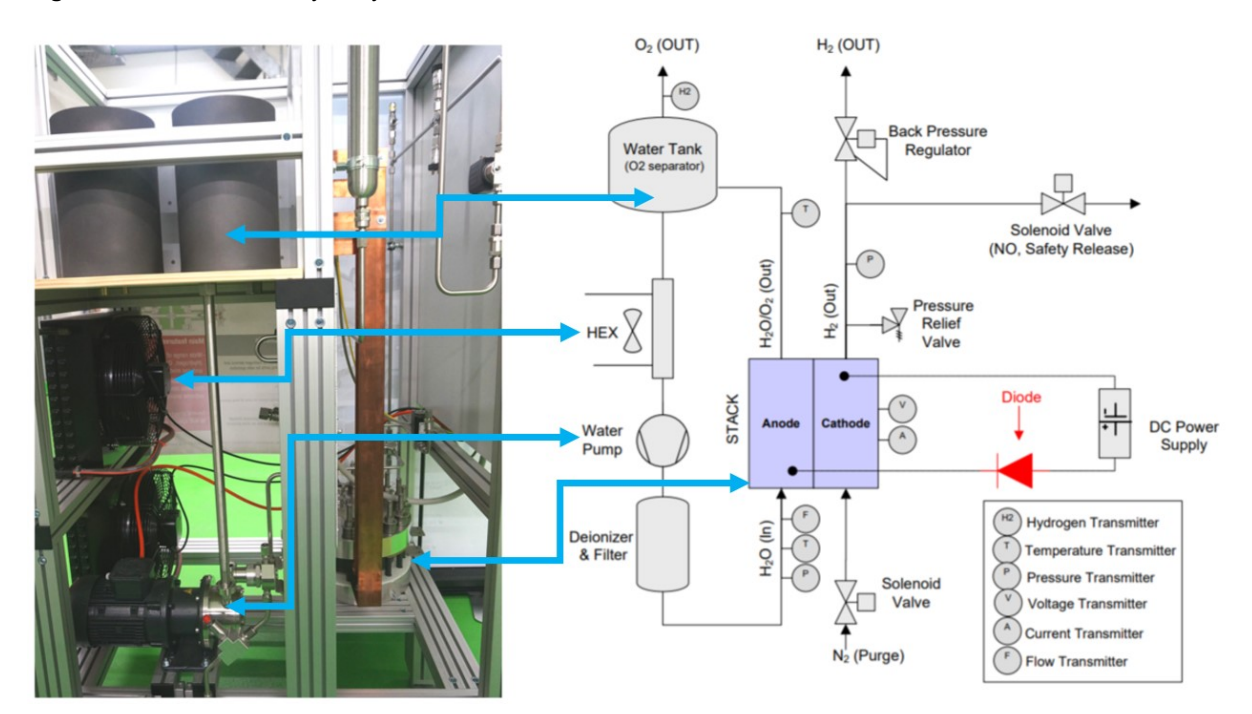


Figure 9 - Alkaline electrolysis system



**Figure 8** -Minimal system configuration for the PEM stack (from Giner manual) and picture of the installed system.



For the alkaline electrolyser, we could mention the following design changes:

- Installation of a hydrogen washer (after condensate tanks). Thanks to this no trace of KOH are detected in the valves
- Proportional operation of the electrolyte cooling system with a winter and summer operating mode
- Optical sensor after drain valves instead of timers, and removal of catch pot reinjection
- Decoupling of heat exchangers to reinforce the cooling efforts on the hydrogen flux
- 20% NaOH replaced by KOH for better conductivity
- Programmation of a warm standby mode for a faster ON/OFF response time
- Original water chiller (Friulair, Italy), replaced with a higher quality (Huber, Germany), which could be shared with the PEM electrolyser.
- Multiple power meter installation to monitor auxiliaries' consumptions.
- Centrifugal electrolyte pump replaced by magnetic coupled version

After discussion with the original supplier, additional stacks were delivered as a compensation and thus we had the opportunity to open a used stack and to analyze the cell characteristics (see **Figure 10Figure 10** and **Table 2**).







Figure 10 - Alkaline stack replacement and disassembly



	PEM	Alkaline
Number of cells	14	2 x 115
Active surface area	300 cm <sup>2</sup>	370 cm <sup>2</sup> (22.5 cm diameter minus the orifices)
Length between end plates	58 mm	703 mm
Cell thickness	4.1 mm	6.1 mm
Membrane thickness	-	1.3 mm (dry)
Bipolar plate thickness	-	0.6 mm

Table 2 - Cell characteristics comparison

#### Control system

Multiple PLCs from Siemens (S7 1200 series) were installed to control, automate, and record the data from the 4 systems constituting the hydrogen production and storage unit. While the water purification system works independently based on the pressure in the reservoir (set to 5 bar). The hierarchy of the system and the data exchanges are summarized in **Figure 11**.

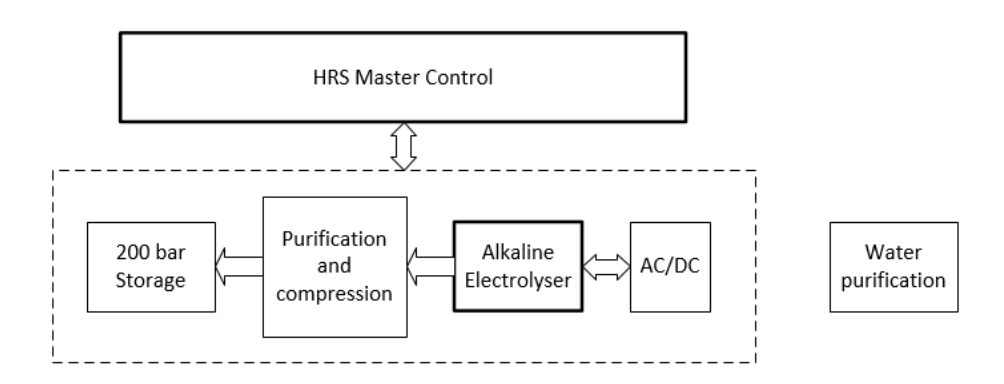


Figure 11 - Overview of the PLCs installed in the demonstrator and corresponding data exchanges

We can describe the typical working sequence of the alkaline electrolyser as follows:

- **Start:** The start button is pressed with a current set point, typically 70 to 115 A. (optional: a preheating of the electrolyte can be turned on before)
- **Pressurization:** Nitrogen is used to bring the system to 10 bar. The balance between the two reservoirs is regulated, and the chiller is started.
- Inertization: for a period of 3 min, a flux of N<sub>2</sub> at 10 bar is used make sure the system is inert.
- **Purge:** a current limited to 70 A is applied to the stacks to bring the electrolyte to a nominal working temperature of 52.5°C without applying a too high cell voltage. During this period the nitrogen present is the system has to be purged for 8 min. The gases produced are vented.
- Production: the entered current set point is finally applied on the stacks. The electrolyte level is adjusted continuously with water injection and regulating valves. A PID ensures the temperature control of the electrolyte. The purification and compression system is also started at this step. The current set point can be changed at any time.



- **Stop:** When the stop button is pressed, first the compression and purification system is turned off and closed, and then the current supply to the stack is stopped.
- **Inertization and cooling:** for a period of 5 min, a flux of N<sub>2</sub> at 10 bar is used to make sure the system is inert. The electrolyte is cooled down to 30°C, using the maximum turning speed of the fans.
- **Depressurization:** the pressure is lowered step by step with 1 min intervals, to ensure a homogeneous desorption of the gas in the electrolyte
- Once the system is fully depressurized, and the electrolyte cooled down. The whole system is turned off (pumps, fans, valves).

## **Purification and storage**

The goal of the hydrogen produced in the demonstrator is to be used in fuel cell for mobility purposes. Therefore, it has to fulfil the purity requirements specified in SAE J2719 [4]. The main pollutant expected with water electrolysis is water. While purification systems are usually shipped together with the electrolyser, it was decided, for more flexibility, to design and built the system in-house.

The purification system operates at 40 bar and is combined with the first step of compression for the alkaline electrolyser. It is made of two 1 gal. reservoirs filled up with 2.77 kg of molecular sieves each (Sigma Aldrich 4 A, beads 8-12 mesh). It is working on the pressure swing principle with a vacuum regeneration. An access to capture gas samples is installed at the inlet of the DLE-15-2 booster. Alternatively, the manifold installed can be connected to a commercial hydrogen bundle, when the local hydrogen production is out of service. The picture and technical sketch of the system are presented in **Figure 12** and **Figure 13**.



Figure 12 - Purification and compression system



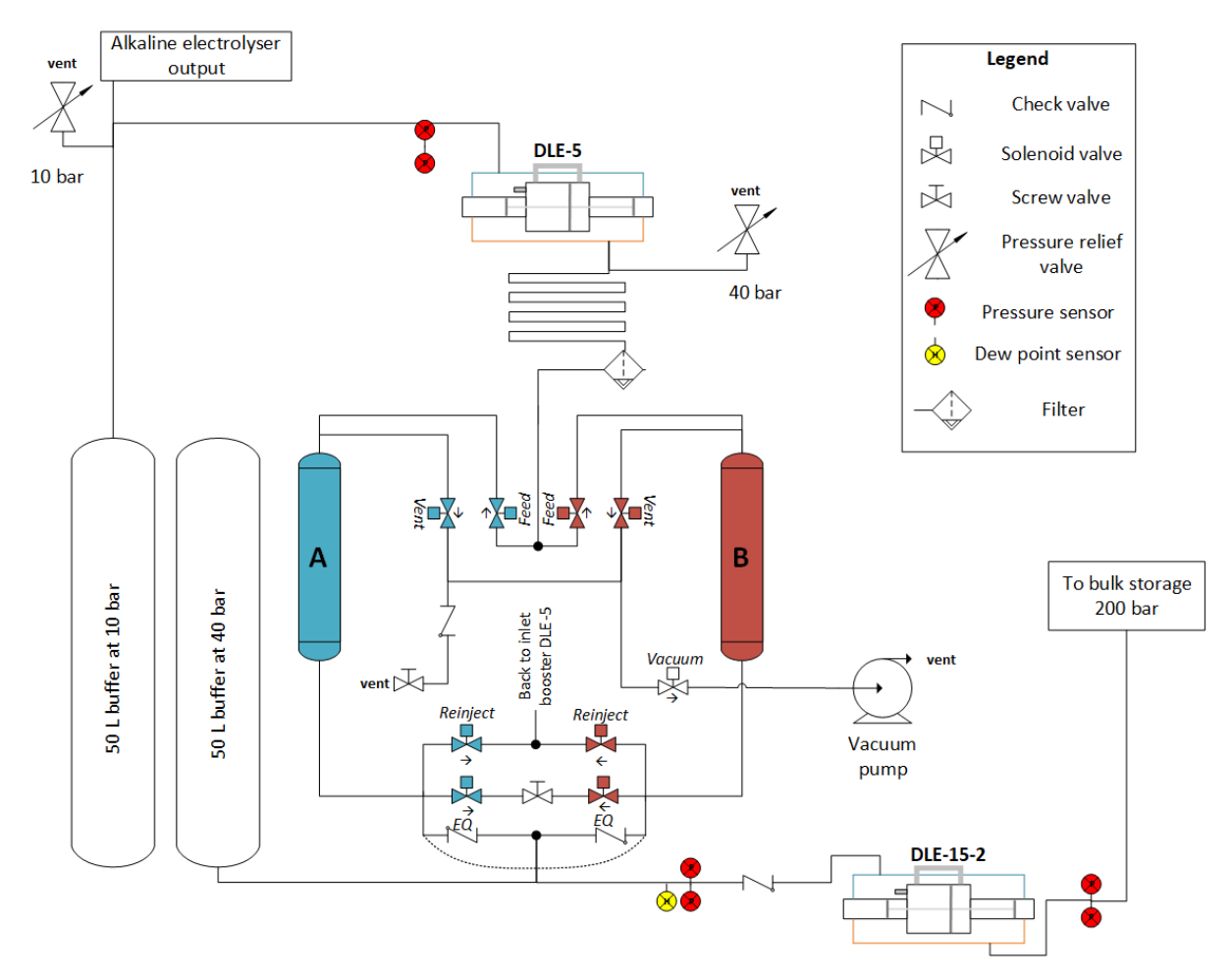


Figure 13 - Pressure swing system for hydrogen purification and compression

It was observed, during the initial inertization of the system, that nitrogen is also adsorbed on the beads. This is particularly interesting during the first minutes of operation, were some nitrogen traces can still be present in the hydrogen flux.

Because the compression speed of the boosters is linked to the inlet pressure, the outlet pressure and the pressure of the compressed air, it was particularly challenging to manage these dynamics. Indeed, the equilibrium and reinjection phases have an influence on the inlet pressure of DLE-5. In addition, when the operating set point of the electrolyser is changed, the speed of compression must be adapted accordingly. The compressed air input is thus controlled with a motorized ball valve, however traditional PID with automated parameter tuning cannot be implemented. A non-linear control function taking into account the hysteresis behaviour of the motor, was therefore manually implemented.

An active cooling might be required for full speed production during summer time, or the maximum working pressure of the supply storage cannot be reached without exceeding the temperature limits of the gas boosters.



The supply storage for the HRS is made of three industrial storage bundles divided in six sections of 300 L. The usable pressure window is comprised between 80 and 200 bar and is determined by the HRS compressor (Maximator DLE 30-2, Germany). It defines a usable storage capacity of 15 kg of H<sub>2</sub>.

## Measurements and performance

We have observed a poor reliability of several sensors and auxiliaries and we changed some systems accordingly:

- Continuous level sensors in the gas separator: changed twice. Redundancy ensured with optical sensors.
- Optical sensor in hydrogen washing system: failed once.
- Original KOH pump: failure detected with a flow sensor. Replaced with a magnetic coupled version, more suitable for operation in alkaline media.

A typical operation of the alkaline electrolyser is presented in **Figure 14**. 30 minutes after the start sequence, the system reached its nominal conditions. The current applied on the stacks was 100 A, the inlet temperature of the electrolyte in the stacks was regulated at 52.5 °C and the outlet was at around 66°C.

During 180 minutes of production, two 300L storage banks were partially refilled, for a total mass of hydrogen produced of 2.32 kg (8.7 Nm<sup>3</sup>/h <sup>5</sup>). We switched from one bank to the other 135 min after the start sequence. The maximum hydrogen production of 10 Nm<sup>3</sup>/h can be reached at 115 A.

The average DC, AC, and auxiliaries power consumptions were respectively 50.4 kW, 53.3 kW and 2.7 kW. Thus we obtain a consumption of 5.8 kWh/Nm³ (DC) and 6.4 kWh/Nm³ (AC and auxiliaries). These values are in line with the literature [5]. The supplier announced respectively 5.2 and 5.5 kWh/Nm³. The chiller was probably not included in the auxiliaries' consumptions from McPhy (ca + 0.11 kWh/Nm³). And we noticed a metallic deposit on the membranes (see **Figure 10**) which may increase the cell voltage. Indeed, compared to the early phase of the project, a 0.1V penalty per cell was measured. However, the announced values seem unrealistic considering that we have replaced almost all auxiliaries and operating routines with more energy efficient alternatives. The cell separator is one of the main drivers for the poor efficiency. Based on the volume of water collected after the deoxo, we suspect a high oxygen crossover.

The purification and compression system fulfilled the design objectives with only 0.3 ppm of water after purification. The air compressor was consuming 14 kW in average. This is less than 50% of its nominal power, which was designed for a simultaneous operation of the 4 gas boosters of the demonstrator. Because an intermediate media, compressed air, is used, the energy losses for this compression step are high. In addition, the long-term operation of gas booster has to be avoided, because maintenance intervals of 20 000 cycles (ca. 12 hours) are recommended. For this demonstrator, reliability and ease of maintenance were favored for this non-electrochemical step. For a better energy efficiency in industrial scale applications, membrane or piston compressors can be used. We can mention that the compressor installed in the future mobility demonstrator from EMPA consumes 7.2 kWh/Nm³ [6].

<sup>5 0.0898</sup> kg of H<sub>2</sub>/Nm<sup>3</sup>



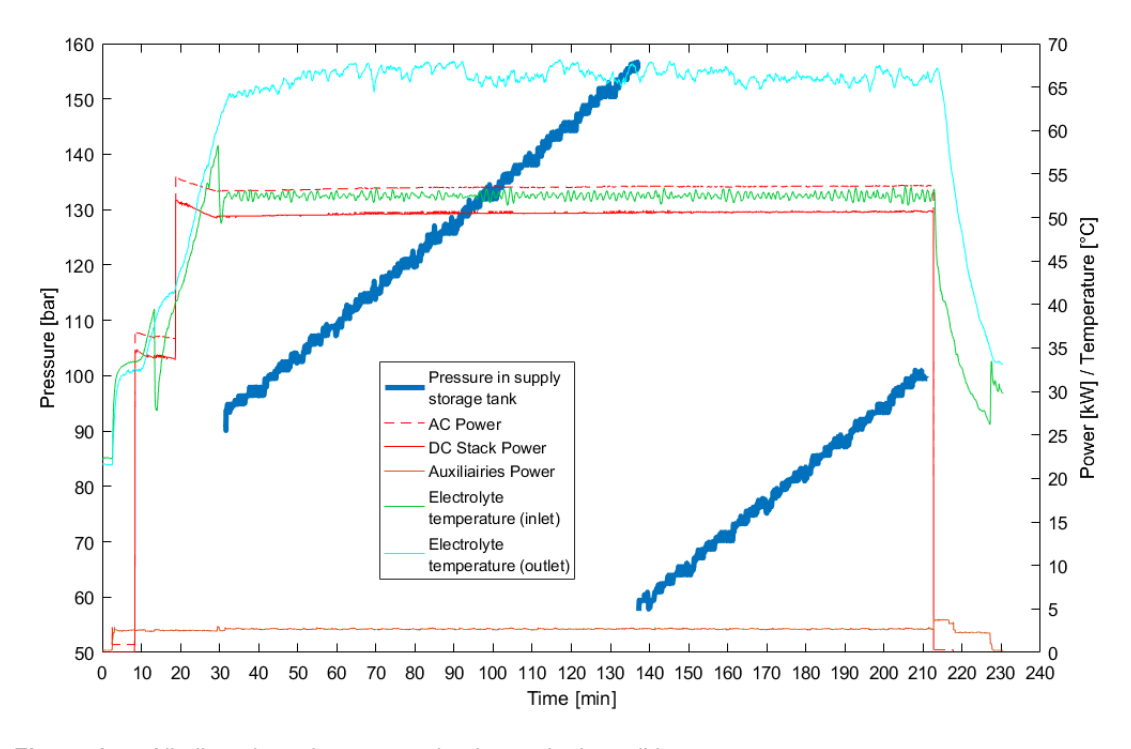
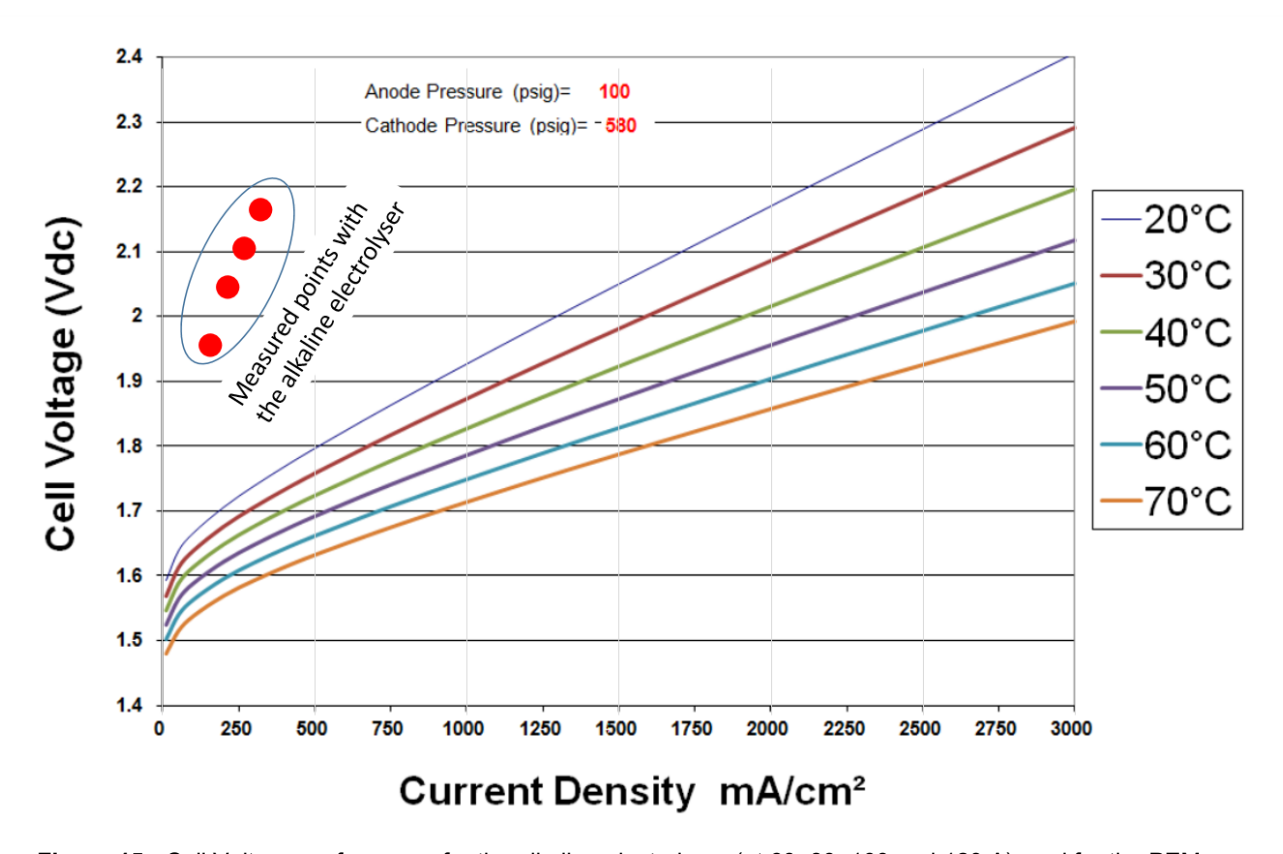


Figure 14 - Alkaline electrolyser operation in nominal conditions

Current set points in the range of 60 to 120 A have been tested and the values are reported on the polarization curve of the PEM in **Figure 15**. Unfortunately, the extensive work on the alkaline electrolyser didn't leave enough time to operate the PEM system within the project timeframe. The maximum production rate with the PEM should be 5.1 Nm³/h with a stack energy consumption of 4.9 kWh/Nm³. A 15% efficiency gain can thus be reported on the DC side compared to the alkaline electrolyser, however almost all these gains are offset by the losses of the power supply as mentioned in subsection 0. EMPA reported a 52% system efficiency based on the LHV (5.8 kWh/Nm³) for the PEM electrolyser installed in the MOVE demonstrator [6]. For a real energy efficiency advantage of the PEM, it should be operated with lower current densities, which is not optimal in terms of CAPEX.





**Figure 15** - Cell Voltage performance for the alkaline electrolyser (at 60, 80, 100 and 120 A), and for the PEM (from Giner Manual)



## Hydrogen compression and filling

## **Compression system**

Four compression steps are required between the alkaline electrolyser output at 10 bar and the fueling nozzle at 700 bar. The first two steps are realized within the purification and compression system presented in subsection 0. The last two stages are realized within the HRS container represented in **Figure 16**. This container is supplied with hydrogen coming from the supply storage at 200 bar.



Figure 16 - Hydrogen refilling station container with cascade system

The different steps characteristics and the operating conditions of the compressors are summarized in **Table 3** and the whole set-up can be recalled from **Figure 1**.

Model	Displacement Volume (cm³)	Inlet Pressure	Outlet Pressure	Maxi- mum Pressure ratio	Source Tank	Destination Tank
DLE-5	746	10 bar	40 bar	5	1 x 50 L	1 x 50 L
DLE-15-2	244	40 bar	100-200 bar	30	1 x 50 L	6 x 300 L
DLE-30-2	120	100-200 bar	200-500 bar	60	6 x 300 L	4 x 50 L
DLE-75-2	50	200-500 bar	300-700 bar	150	6 x 300 L	4 x 50 L or vehicle

 Table 3 - Technical specifications and implementation of gas boosters used within the demonstrator



All stages are performed with air driven gas boosters from the company Maximator (Germany). This technology, using compressed air as driving force, is particularly robust and safe to operate. The installation and maintenance operations can be realized with ready-to-use kits and, most of the time, do not require the intervention of external technicians. The compressed air is supplied with a 37 kW screw compressor from Kaeser, connected to a 900 L buffer storage. This compressor is equipped with a heat recuperation system, used to heat the building.

In order to fully characterize the gas boosters, they are all equipped with the following set of sensors:

- Inlet and outlet pressure
- Inlet and outlet temperature
- Mass flow meter for the compressed air
- Counter for the number of cycles

Rupture discs are installed at the outlet to prevent damages.

A typical operation of the booster DLE-30-2 is presented in Figure 17.

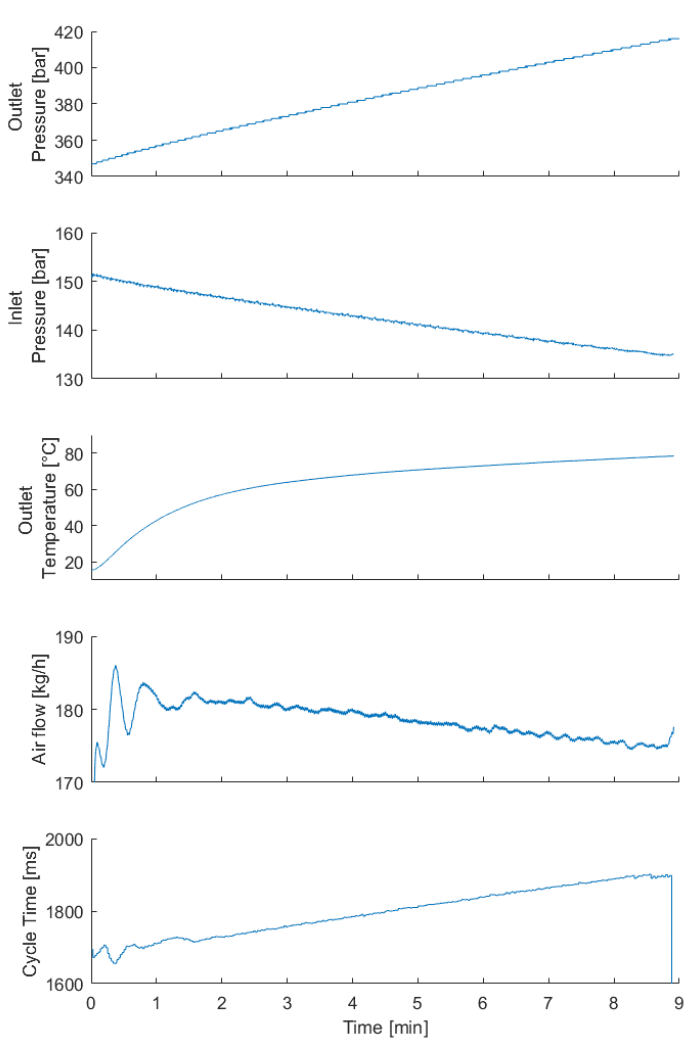


**Figure 17** - Compression from supply storage (300L) to high pressure cascade (2x50L) with a DLE-30-2 gas booster



A model, based on geometrical considerations from **Figure 18**, was developed in order to predict the outlet temperature, the cycle time at full speed and to investigate volumetric efficiencies.

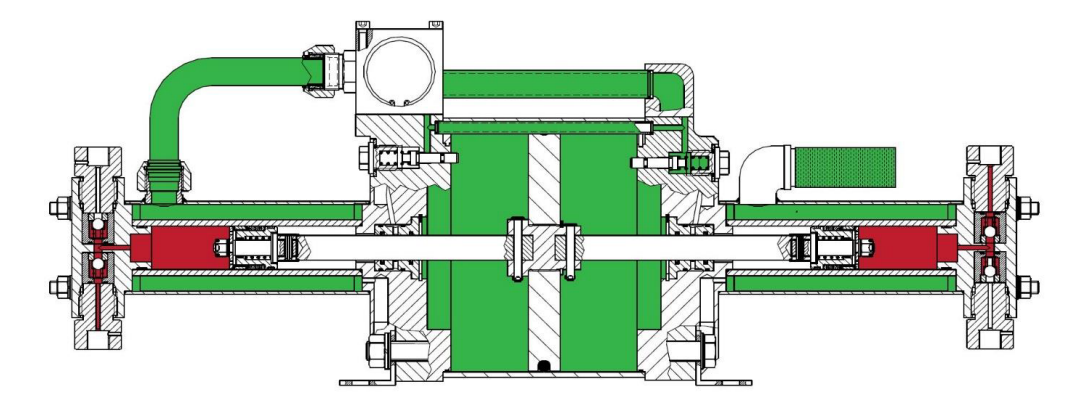


**Figure 18** - Cross sectional view of a air driven gas booster. Compressed air in the green region and hydrogen in the red region (from Maximator)

A linear relationship was found between the cycle time and the pressure difference between the inlet and the oulet of the booster. Regarding temperatures, it was found that the ratio between outlet and inlet pressures should be maintained below 5 to stay within the temperature limits defined by Maximator.

## Hydrogen refueling station

The station was initially designed and built to refill the 70 L tank of the Swiss Hydrogen Kangoo at 350 bar [7] in less than 5 min. It was successfully achieved, automated and repeated multiple times, with a user- friendly interface as presented in **Figure 19** and **Figure 21**.

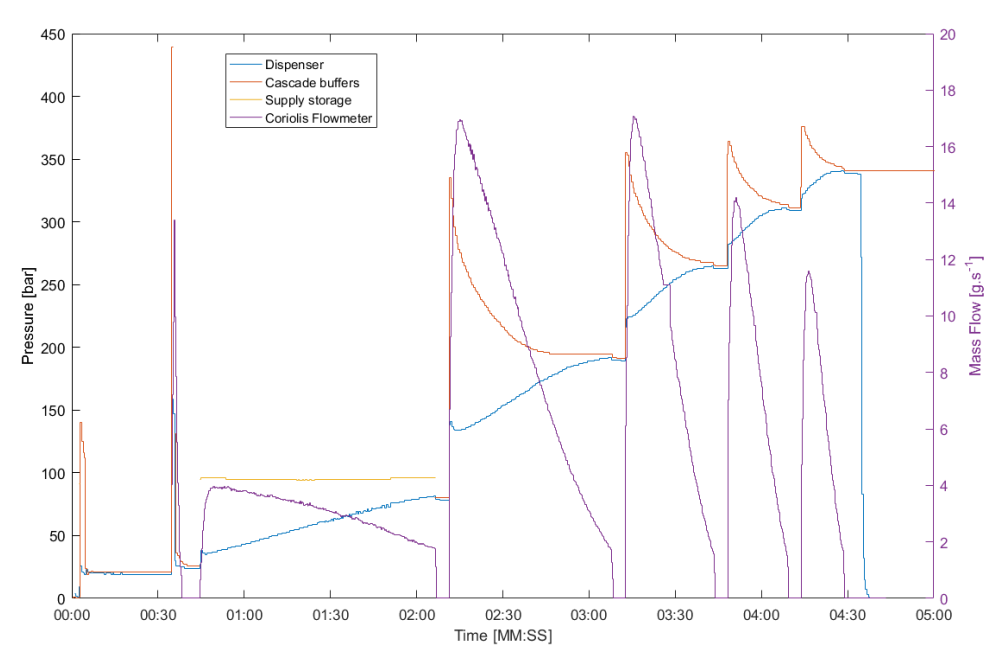


Figure 19 - Refueling cascade for the 70 L reservoir of the Swiss Hydrogen Kangoo





Figure 21 - User friendly interface for the automated 350 bar refueling sequence

It became rapidly evident that the station capability could easily be upgraded and used to refill the Hyundai ix35 Fuel Cell at 700 bar. Although the standard 5 minutes protocol with precooling [8] cannot be applied. Indeed, another stage of high-pressure cascade at 850-900 bar would be required together with a high-pressure heat exchanger and an electro-pneumatic pressure regulator. Alternatively, we decided to use the DLE-75-2 booster directly connected to the 700 bar filling nozzle. The temperature evolution is monitored *via* infra-red communication [9]. As a result, with a sufficient pressure in the supply storage, vehicles with up to 8 kg of hydrogen on-board have been refilled at 700 bar (which exceeds the capacity of all passenger cars available today). Even though this very specific refilling sequence is significantly longer, and is not automated, it offers an interesting and cost-effective back-up solution. The company GreenGT<sup>6</sup>, based in Aclens (VD), contacted us for several refillings of their GreenGT H2 racing prototype. The refilling sequence implemented is presented **Figure 20**.

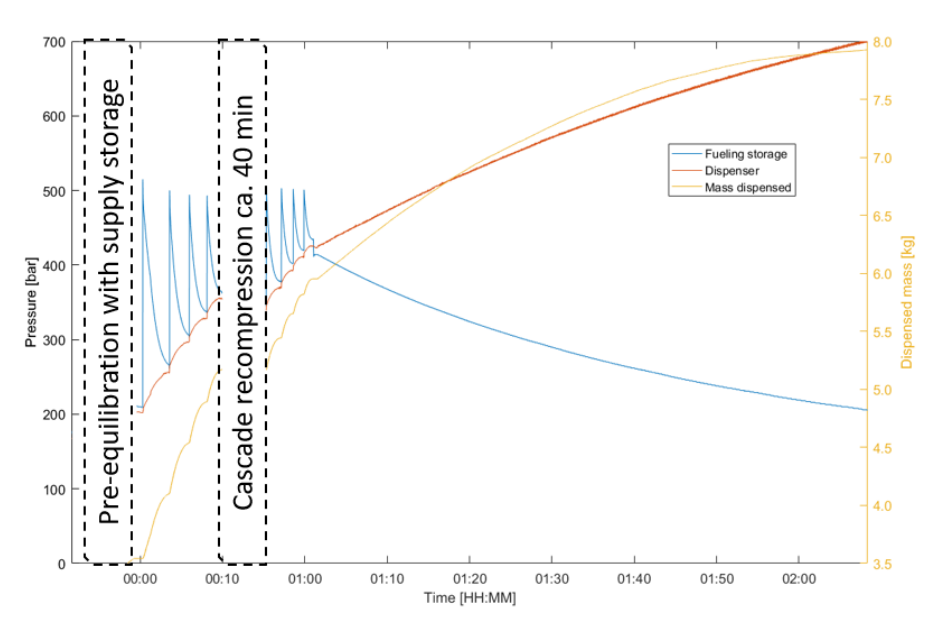


Figure 20 - Hydrogen fueling procedure for the GreenGT H2

<sup>6</sup> http://greengt.com/



Additionally, the high flexibility of the station allowed us to test high pressure cylinders for leakage and geometrical deformations, and to recycle the hydrogen to refill the Hyundai ix35 as presented in **Figure 22**.



Figure 22 - High pressure tank testing with hydrogen recycling



## Conclusions and outlook

This demonstrator, conceived and built around electrochemical devices, has highlighted the major importance of an appropriate balance of plant for system integration and in particular of power electronics and control systems. Costs, implementation timeframes, system reliability and system energy efficiency are highly affected by the cumulative contribution of all auxiliaries.

In three year period, a hydrogen refilling station with on-site electrolysis was designed, build and put into service. A DC charger coupled to the DC Bus of a VRFB was installed. Radical design choices, oriented towards exhaustive data collection and robust components, were made when off the shelf solutions did not offer satisfactory specifications or behaviour in operation. Hence, a unique know-how was developed on both hardware and software for water electrolysis, hydrogen purification and compression, and VRFB management. Large sets of data have been collected and contributed to a better understanding of the processes occurring in grid to mobility set-ups.

The high versatility of the installation was used to refill small cargos vans (Swiss Hydrogen Kangoo), large hydrogen SUVs (Hyundai ix35 Fuel Cell) and race prototypes (Green GT H2). In addition, several public users benefited from the electric charger, using both AC and DC interfaces.

This project generated interest above our expectations. We have received multiple requests to share our technical expertise around electric and hydrogen mobility and we have been involved in several working groups in particular with the Canton du Valais and the SIG. Interestingly, the station was also used outside of the initial project scope with tank testing and refillings for Green GT, and some early adopters looking for an HRS in the region.

We hope that the list provided in Appendix 0, in addition to the technical drawings, will help other groups to design and engineer their own systems. In Martigny, after two successful projects supported by the SFOE, the facility is now fully equipped to host future demonstrators. The data collection will be pursued, and will contribute to other collaborative projects such as the Coherent Energy Demonstrator Assessment (CEDA). Primary data for VRFB and alkaline electrolyser stacks materials and components is available on request to improve life cycle inventories databases. The equipments will be also used for education, with two master students from EPFL hosted in Martigny in 2019. Additional research will be conducted on BMS for VRFB, pursuing our exchange of expertise with the supplier. Finally, the knowhow developed, in addition to the high level of implication of local partners, may generate new ambitious projects in a near future.



## **Acknowledgments**

The project team would like to address its thanks to the Swiss Federal Office for the support and funding of the project.

We also express our gratitude to all the project partners involved from the CREM (Olivier Dumas, Jakob Rager, Vincent Roch, Numa Gueissaz, Pablo Puerto), from Sinergy (Patrick Pralong, Jonathan Carron), from LEPA (Heron Vrubel, Frederic Gumy, Veronique Amstutz, Alberto Battistel, Christopher Dennison, Danick Reynard, Declan Bryans), the mechanical workshops from EPFL Valais and EPFL Lausanne, and the EPFL Direction for their support (Provost P. Gillet, VP E. Marclay and Mr. M-A Berclaz).

We truly appreciate the continuous support from the city of Martigny, and the staff of the water treatment plant with whom we have shared the infrastructure since 2014.

## **Publications and outreach**

## Journal papers

#### Published

- R. Frischknecht *et al.*, "LCA of mobility solutions: approaches and findings—66th LCA forum, Swiss Federal Institute of Technology, Zurich, 30 August, 2017," *The International Journal of Life Cycle Assessment*, vol. 23, no. 2, pp. 381–386, Feb. 2018.
- Y. Ligen, H. Vrubel, and H. Girault, "Mobility from Renewable Electricity: Infrastructure Comparison for Battery and Hydrogen Fuel Cell Vehicles," *World Electric Vehicle Journal*, vol. 9, no. 1, p. 3, May 2018.
- D. Bryans, V. Amstutz, H. Girault, and L. Berlouis, "Characterisation of a 200 kW/400 kWh Vanadium Redox Flow Battery," *Batteries*, vol. 4, no. 4, p. 54, Nov. 2018.

#### Submitted in 2018

- Y. Ligen, H. Vrubel, and H. Girault, "Stochastic modelling of 150 kW EV charging stations and reduction of peak power requirements with local stationary batteries" (developing the work presented in subsection 0)
- D. Reynard, H. Vrubel, C.R. Dennison, A. Battistel and H. Girault, "On-site purification of copper-contaminated vanadium electrolytes using a vanadium redox flow battery" (developing the work presented in subsection 0)

#### To be submitted in 2019

- Y. Ligen and H. Girault, "Compressed air gas booster for hydrogen refilling station: modelling and operation" (based on the work presented in subsection 0)
- Y. Ligen, H. Vrubel and H. Girault, "Dynamic operation of a 50kW alkaline electrolyser and pressure swing purification" (based on the work presented in subsection 0)



#### International conferences

- EEVC 2017, "Megabatteries for fast DC charging and hydrogen production. Fuelling both electric cars and fuel cell cars", March 2017, Geneva, Switzerland
- EVS30, "Infrastructure comparison for battery and hydrogen fuel cell vehicles: Energy footprint from Grid to Mobility", October 2017, Stuttgart, Germany
- EEVC 2018, "Design and operation of a Grid to Mobility Demonstrator Self-sufficiency and self-consumption considerations", March 2018, Geneva, Switzerland
- ECS233, "Redox flow batteries for fast EV charging and for hydrogen production for FCEVs", May 2018, Seattle, USA
- IFBF 2018, site visit organized in Martigny
- EVS 32, "Energy storage to reduce to power requirements and operating costs of fast charging stations", May 2019, Lyon, France

#### In the press and various events

The visibility of the project was also ensured with the participation in various events and several press coverages addressed to a large public, we can list for example:

- Scientific community: LCA Discussion Forum 66, SCCER events, CEDA
- General public, local level: Swiss Mobility Days 2017, Rallye International du Valais 2018, 4 articles in "Le Nouvelliste", conferences and site visits organised for various associations such as Kiwanis, Rotary, Ravel
- General public, national level: RTS "Aujourd'hui la voiture de 2018", 2 radio interviews on RTS
- Students: site visits organized for EPFL association of the chemistry students (ADEC), Eurotech Winterschool, HES
- International visits coordinated by the cantonal office for Economic development and foreign investments



## Références

- [1] Y. Ligen, H. Vrubel, and H. Girault, "Mobility from Renewable Electricity: Infrastructure Comparison for Battery and Hydrogen Fuel Cell Vehicles," *World Electric Vehicle Journal*, vol. 9, no. 1, p. 3, May 2018.
- [2] D. Bryans, V. Amstutz, H. Girault, and L. Berlouis, "Characterisation of a 200 kW/400 kWh Vanadium Redox Flow Battery," *Batteries*, vol. 4, no. 4, p. 54, Nov. 2018.
- [3] H. Girault and V. Amstutz, "Final Report RFB-HY: redox flow battery pilot installation for hydrogen generation and energy storage." Swiss Federal Office of Energy, 30-Jan-2017.
- [4] SAE International, "J2719: Hydrogen Fuel Quality for Fuel Cell Vehicles." Nov-2015.
- [5] T. Smolinka, M. Günther, and J. Garche, "NOW-Studie: Stand und Entwicklungspotenzial der Wasserelektrolyse zur Herstellung von Wasserstoff aus regenerativen Energien," Fraunhofer ISE, 2011
- [6] U. Cabalzar, T. Schildhauer, and C. Schürch, "Final Report Hydrogen production from excess electricity with use in mobility or re-conversion to electricity." Swiss Federal Office of Energy, 27-Nov-2017.
- [7] Swiss Federal Office for Energy SI/501415, "SwissKangooFC: 700 bar Hydrogen fuel cell range extender," 01-May-2017. [Online]. Available: https://www.aramis.admin.ch/Beteiligte/?ProjectID=38237.
- [8] SAE International, "J2601: Fueling Protocols for Light Duty Gaseous Hydrogen Surface Vehicles." Dec-2016.
- [9] SAE International, "SAE J2799, Hydrogen Surface Vehicle to Station Communications Hardware and Software." 2014.



## **Annexes**

## **Supplier specifications of main equipments**

Alkaline Electrolyser: McPhy, McLyzer 10-10

P	arameter	Value	Unit
Num	ber of stacks	2	N/A
	ominal H <sub>2</sub> roduction	10	Nm³/h
	ominal O2 roduction	5	Nm³/h
Ope	ration range	25 to 100	% of the nominal load
Opera	ting pressure	≤ 12	barg
	perating mperature	< 70	°C
Hydr	ogen quality	$0.5~\%$ of $O_2$ in $H_2$ and water saturated (about 1200 ppm $H_2O$ )	N/A
Di	mensions	1.5 x 1.5 x 2	m (LxWxH)
	Mass	ca. 850	kg
nance			Wh/Nm³ (DC power @ nominal flow rate)
Performance			Wh/Nm³ (AC power @ nominal flow rate)



## PEM Stack: Giner, Merrimack 14 cells, 900 A

Characteristics	Units	Rating	Notes
H <sub>2</sub> Production (Max)	Nm³ H <sub>2</sub> /hr/Cell ( kg H <sub>2</sub> /hr/Cell)	0.37 (0.033)	Example: A Merrimack stack with 85 cells will produce 31.8 Nm³-H₂/hr (2.84 kg-H₂/hr) at maximum current
H <sub>2</sub> Production (Min)	Nm³ H₂/hr/Cell ( kg H₂/hr/Cell)	0.036 (0.0032)	Example: A Merrimack stack with 85 cells will produce 3.1 Nm³-H₂/hr (0.27 kg-H₂/hr) at minimum current
Current (Max)	Amp (DC)	900	Current Density Range : 300-
Current (Min)*	Amp (DC)	90 A	3,000 mA/cm <sup>2</sup>
Cell Voltage**	Voltage(DC)/Cell	1.94 (BOL) 2.40 (EOL)	BOL = Beginning of Life EOL = End of Life
Maximum H₂ Operating Pressure***	bar(gauge) (psig)	40 (580)	
Maximum Inlet Operating Temperature	°C (°F)	70 (158)	Desirable Temp 65 – 70 °C

<sup>\*</sup>At maximum differential pressure (Current below 90A is possible at lower operating pressures. Contact Giner, Inc. Engineering for further details

<sup>\*\*\*</sup> Hydrogen pressure should be above oxygen pressure

Stack Size*	Dimen	sion "C"	Dimen	sion "D"	Dimen	sion "H"	Mas	s, M	Est. Dry Capac.
(Cells)	(mm)	(inches)	(mm)	(inches)	(mm)	(inches)	(kg)	(lbm)	(Farad)
1	3.6	0.14	47.2	1.86	191	7.5	91	200	0.0649
5	18.0	0.71	48.0	1.89	207	8.1	93	205	0.0130
14	58	2.265	95	3.75	292	11.5	100	218	0.0464
60	216	8.52	98.6	3.88	454	17.9	132	290	0.0011
81	292	11.5	114	4.48	545	21.5	145	321	0.0008
85	302	12.0	120	4.74	565	22.3	148	327	0.0008
97	350	13.8	127	5.0	618	24.3	156	345	0.0006
250	902	35.5	290	11.4	1,331	52.4	268	590	0.0003

<sup>\*</sup> Additional stack sizes available. \*\*All Dimensions approximate within +/-6mm (+/-0.25 inches)

Power supply from Magna Power

Model TSC 32-900. Efficiency: 86 %

<sup>\*\*</sup>At maximum current (900 A), temperature (70°C), and pressure (40 barg). Lower operating temperature increases cell voltage



## Gas booster: Maximator, DLE-5, DLE-15-2, DLE-30-2, DLE-75-2

Main         Max         pressure         end perssure in potessure in potessure in potessure in page         end perssure in potessure in potessure in potessure in potessure in page         curd mode of the page         page         bar (psi)         double stroke infeature or curin         cycle         request         feature or curin         request         feature or curin         request         feature or curin         request         feature or curin	Pressure	Com-	Sucti	Suction pres	sure		Max. outlet	tlet	Formula for max.	Displa	Displacement	Max	Connections	ons	Мах.	Weight	
1.10   0   0   0   20   20   20   20   20	atio i,/ i,)	pression ratio*	Min pA bar	psi	Max bar	psi	pressure pB bar	i psi	end pressure in bar (psi)	volume double cm³	e per estroke cu.in	cycle frequency 1/min		Outlet	operating pressure °C	kg	
1:50   2   29   67   75   75   75   75   75   75   75	:2	1:10	0	0	20	290	20	290	2*pL	922	56.26	100	1/2 BSP	1/2 BSP	09	15	
1.20   15   129   14   129   14   129   14   129   14   14   14   14   14   15   14   15   14   15   14   15   14   15   14   15   14   15   14   15   14   15   14   15   14   15   14   15   14   15   14   15   14   15   14   15   14   15   15	:5	1:15	2	53	20	725	20	725	5*pL	373	22.76	110	1/2 BSP	1/2 BSP	09	15	
1:20   35   508   500   4;550   30° pt   450   30° pt   60   366   130   14459   14869   100   13   14159   14169   14169   100   13   14150   14169   14169   14169   100   13   14150   14169   14169   14169   100   13   14150   14169   14169   100   13   14150   14169   14169   100   14160	: 15	1:20	7	102	150	2,175	150	2,175	15*pL	122	7.44	130	1/4 BSP	1/4 BSP	100	13	Į.
1.10   1.10	1:30	1:20	15	218	300	4,350	300	4,350	30*pL	09	3.66	130	1/4 BSP	1/4 BSP	100	13	
1:10   1.0	1:75	1:20	35	208	750	10,875	750	10,875	75*pL	25	1.53	130	1/4 BSP	1/4 BSP	100	13	
1:15   2   29   10   1459   100   1450   1450   57pL+ph   244   1489   120   1188P   1188P   100   18   11.20   11.20   13   218   600   21.30   21.350	1:2	1:10	0	0	40	580	40	580	2*pL + pA	1844	112.53	06	1/2 BSP	1/2 BSP	09	20	
1.20   1.2   10.2   30.0   4,350   3,70   1,70   1,70   1,70   1,70   1,85   1,148   1,488	1:5	1:15	2	29	100	1,450	100	1,450	5*pL + pA	746	45.52	110	1/2 BSP	1/2 BSP	09	20 ,	
1.20   35   58   580   8,700   600   8,700   30°pL + pA   120   73.2   120   14.85p   14.85p   100   18   18   11.20   12.50   15.50	1:15	1:20	7	102	300	4,350	300	4,350	15*pL + pA	244	14.89	120	1/4 BSP	1/4 BSP	100	8	
1:20   35   508   1;500   21;750   1;500   21;754   25   14   14	1:30	1:20	15	218	009	8,700	009	8,700	30*pL + pA	120	7.32	120	1/4 BSP	1/4 BSP	100	8	,
1. 1. 1. 2   0   0   0.8   0.4   1. 450   1. 4	1:75	1:20	35	208	1,500	21,750	1,500	21,750	75*pL + pA	20	3.05	130	1/4 BSP	1/4 BSP	100	18	
1.45   2   29   1,6°PL   300   4,350   15°PL+3°PA   373   22.76   110   11,285   1485P   100   19   19   1.2   1	1:2 / 1:5	1:25	0	0	0.8*PL		100	1,450	5*pL + 2.5*pA	922	56.26	100	1/2 BSP	1/2 BSP	09	20	
1.30   2   29   1.5°   1.0   1.2   1.0   1.2   1.0   1.2   1.0   1.2   1.0   1.2   1.0   1.2   1.0   1.2   1.0   1.2   1.0   1.0   1.2   1.0   1.2   1.0   1.0   1.2   1.0   1.0   1.2   1.0   1.0   1.2   1.0   1.0   1.2   1.0   1.0   1.2   1.0	1:5 / 1:15	1:45	2	53	1,6*PL		300	4,350	15*pL + 3*pA	373	22.76	110	1/2 BSP	1/4 BSP	100	19	
	1:5 / 1:30	1:90	7	53	0,5*PL		009	8,700	30*pL + 6*pA	373	22.76	110	1/2 BSP	1/4 BSP	100	19	
75         1:100         7         102         2,5°PL         1,500         21,75°D         75°PL+2,5°PA         60         3.66         120         144 BSP         100           7:5         1:50         1:5         1:5         1:5         1:5         1.2         144 BSP         144 BSP         140         100         1450         10°PL         375         6.26         100         112 BSP         172 BSP         60           1:15         4         58         100         1,450         10°PL         332         22.76         110         112 BSP         178 BSP         100           1:20         20         60         4,350         30°PL         1750         10°PL         48         10°PL         110         112 BSP         148 BSP         100           1:20         20         60         3,50         60         8,700         60°PL         60°PL         60°BC         3.66         120         114 BSP         148 BSP         148 BSP         100           1:20         20         60         1,450         10°PL         4*PL         125         5.	1:15 / 1:30	1:40	7	102	7,5*PL		009	8,700	30*pL + 2*pA	122	7.44	120	1/4 BSP	1/4 BSP	100	19	
1:15   1.5	1:15 / 1:75	1:100	7	102	2,5*PL		1,500	21,750	75*pL + 5*pA	122	7.44	120	1/4 BSP	1/4 BSP	100	19	
1:15   4   58   100   1,450   10°   10°   11°   11°   11°   15°   11°	1:30 / 1:75	1:50	12	218	12*PL		1,500	21,750	75*pL + 2.5*pA	09	3.66	120	1/4 BSP	1/4 BSP	100	19	
1:15   4   58   100   1,450   100   1,450   10 <sup>4</sup> pL   313   22.76   110   1,12 B5   1,12 B5   1,12 B5   60   1,12 B5   1,12	1:4	1:10	0	0	40	580	40	580	4*pL	922	56.26	100	1/2 BSP	1/2 BSP	09	22	0
1:20   10   145   300   4,350   300   6,350   30°pL   120   7.44   110   14.485P   14.485P   100   100   11.20   20   290   600   7,250   600   8,700   60°pL   60   3.66   120   14.485P   14.485P   100   14.885P   14.885P   100   14.885P   14.885P   100   14.885P   14.885P   100   14.885P   14.885P   14.885P   100   14.885P   14.885	1:10	1:15	4	28	100	1,450	100	1,450	10*pL	373	22.76	110	1/2 BSP	1/2 BSP	09	22	
1:20   20   290   600   7;250   600   8;700   60*pL   60   3:66   120   1/4 BSP   1/4 BSP   100   1.50	1:30	1:20	0	145	300	4,350	300	4,350	30*pL	122	7.44	110	1/4 BSP	1/4 BSP	100	20	
1:20         45         653         1,500         21,750         150*pL         25         153         120         1/4 BSP         144 BSP         144 BSP         100           1:11         0         0         40         580         4*pL + pA         1844         112.53         90         1/2 BSP         172 BSP         100           1:15         4         58         100         1,450         100         1,450         10*pL + pA         48.52         100         1/2 BSP         172 BSP         60           1:120         4         58         100         1,450         10*pL + pA         44.55         100         1/2 BSP         172 BSP         60           1:20         20         600         8,700         60°PL + pA         120         7.32         100         1/4 BSP         144 BSP         100           1:20         20         60         8,700         60°PL + pA         50         3.05         10         1/4 BSP         144 BSP         100         1/4 BSP         100           1:20         1:20         43         50         15°PL + pA         3.05         10         1/4 BSP         144 BSP         100         1/4 BSP         100         1	1:60	1:20	70	290	009	7,250	009	8,700	1d*09	09	3.66	120	1/4 BSP	1/4 BSP	100	20	-0.0
1:15         4         4         4*pl + pA         1844         112.53         90         17.2 BSP         17.2 BSP         60           1:15         4         58         100         1,450         100         1,450         10*pl + pA         746         45.52         100         17.2 BSP         17.2 BSP         60           1:20         10         1,450         100         1,450         10*pl + pA         746         45.52         100         17.2 BSP         100           1:20         20         600         8,700         60°         8,700         60°*pl + pA         732         100         1/4 BSP         114 BSP         114 BSP         114 BSP         100           1:20         20         600         8,700         60°*pl + pA         70         732         100         1/4 BSP         100           1:20         21,750         1,500         1,750         150*pl + pA         50         3.05         100         1/4 BSP         100           1:20         4         65         1,500         1,500         1,450         10°*pl + 2.5*pA         50.2         50.26         90         1/2 BSP         100           1:20         2         2	1:150	1:20	45	653	1,500	21,750	1,500	21,750	150*pL	25	1.53	120	1/4 BSP	1/4 BSP	100	20	
1:15         4         58         100         1,450         10^4pL+pA         746         45.52         100         17.2 BSP         17.2 B	1:4	1:1	0	0	40	580	40	580	4*pL + pA	1844	112.53	06	1/2 BSP	1/2 BSP	09	25	
1:20         10         145         300         4,350         30°pl + pA         244         14.89         100         1/4 BSP         1/4 BSP         100         10	1:10	1:15	4	28	100	1,450	100	1,450	10*pL + pA	746	45.52	100	1/2 BSP	1/2 BSP	09	25	
1:20         20         290         600         8,700         60 <sup>4</sup> pL + pA         120         7.32         100         1/4 BSP         144 BSP         144 BSP         140 BSP         100           1:20         45         653         1,500         21,750         1,570         150 <sup>4</sup> pL + pA         50         3.05         100         1/4 BSP         144 BSP         140         100           1:25         0         1,6*PL         100         1,450         10*pL + 2.5*pA         373         22.76         100         1/2 BSP         172 BSP         100           1:45         2         3,2*PL         300         4,350         30*pL + 3*pA         373         22.76         100         1/2 BSP         148 BSP         100           1:40         7         12         2.9         1*pL         600         8,700         60*pL + 6*pA         373         22.76         100         1/2 BSP         144 BSP         100           1:40         7         10         15*PL         600         8,700         60*pL + 2*pA         122         7.44         100         1/4 BSP         100           1:100         7         12         2*pL         10         1/4 BSP         144 B	1:30	1:20	10	145	300	4,350	300	4,350	30*pL + pA	244	14.89	100	1/4 BSP	1/4 BSP	100	23	
1:20         45         653         1,500         21,750         1,570         1,750         1,57	1:60	1:20	70	290	009	8,700	009	8,700	60*pL + pA	120	7.32	100	1/4 BSP	1/4 BSP	100	23	
1:25         0         0         1.6*PL         100         1,450         10*PL+2.5*pA         922         56.26         90         1/2 BSP         1/2 BSP         60           1:45         2         29         3,2*PL         300         4,350         30*pL+3*pA         373         22.76         100         1/2 BSP         1/4 BSP         100           1:90         2         29         1*pL         600         8,700         60*pL+6*pA         373         22.76         100         1/2 BSP         144 BSP         100           1:40         7         102         15*PL         600         8,700         60*pL+2*pA         122         7.44         100         1/4 BSP         144 BSP         100           1:100         7         102         5*PL         1,500         21,750         150*pL+5*pA         122         7.44         100         1/4 BSP         140         100           1:50         2*PL         1,500         21,750         150*pL+2.5*pA         60         3.66         100         1/4 BSP         1/4 BSP         100	1:150	1:20	45	653	1,500	21,750	1,500	21,750	150*pL + pA	20	3.05	100	1/4 BSP	1/4 BSP	100	23	
1:45         2         29         3,2*PL         30         4,350         30*pL + 3*pA         373         22.76         100         1/2 BSP         1/4 BSP         100           1:90         2         29         1*pL         600         8,700         60*pL + 6*pA         373         22.76         100         1/2 BSP         144 BSP         100           1:40         7         102         15*pL         600         8,700         60*pL + 2*pA         122         7.44         100         1/4 BSP         148 BSP         100           1:100         7         102         5*pL         1,500         21,750         150*pL + 5*pA         122         7.44         100         1/4 BSP         140         100           1:50         1:50         21,750         150*pL + 2*pA         60         3.66         100         1/4 BSP         140         100	1:4 / 1:10	1:25	0	0	1.6*PL		100	1,450	10*pL + 2.5*pA	922	56.26	06	1/2 BSP	1/2 BSP	09	25	
1:90         2         29         1*PL         600         8,700         60*pL+6*pA         373         22.76         100         1/2 BSP         1/4 BSP         100         100         1/4 BSP         100 <td>1:10 / 1:30</td> <td>1:45</td> <td>2</td> <td>53</td> <td>3,2*PL</td> <td></td> <td>300</td> <td>4,350</td> <td>30*pL + 3*pA</td> <td>373</td> <td>22.76</td> <td>100</td> <td>1/2 BSP</td> <td>1/4 BSP</td> <td>100</td> <td>24</td> <td></td>	1:10 / 1:30	1:45	2	53	3,2*PL		300	4,350	30*pL + 3*pA	373	22.76	100	1/2 BSP	1/4 BSP	100	24	
1:40         7         102         15*PL         600         8,700         60*pL + 2*pA         122         7.44         100         1/4 BSP         1/4 BSP         100           1:100         7         102         5*PL         1,500         21,750         150*pL + 5*pA         122         7.44         100         1/4 BSP         140         100           1:50         15         218         24*PL         1,500         21,750         150*pL + 2.5*pA         60         3.66         100         1/4 BSP         1/4 BSP         100	1:10 / 1:60	1:90	2	53	1*PL		009	8,700	60*pL + 6*pA	373	22.76	100	1/2 BSP	1/4 BSP	100	24	
1:100         7         102         5*PL         1,500         21,750         150*pL + 5*pA         122         7.44         100         1/4 BSP         1/4 BSP         100           1:50         15         218         24*PL         1,500         21,750         150*pL + 2.5*pA         60         3.66         100         1/4 BSP         1/4 BSP         100	1:30 / 1:60	1:40	7	102	15*PL		009	8,700	60*pL + 2*pA	122	7.44	100	1/4 BSP	1/4 BSP	100	24	
1:50 15 218 24*PL 1,500 21,750 150*pL + 2.5*pA 60 3.66 100 1/4 BSP 1/4 BSP 100	1:30 / 1:150	1:100	7	102	5*PL		1,500	21,750	150*pL + 5*pA	122	7.44	100	1/4 BSP	1/4 BSP	100	24	
	1:60 / 1:150	1:50	15	218	24*PL		1,500	21,750	150*pL + 2.5*pA	09	3.66	100	1/4 BSP	1/4 BSP	100	24	

lbbreviations: pL = Air drive; pA = Suction pressure; pB = Outlet pressure to 100 cy

The maximum permitted outlet pressure is 60 to 100°C. Cooling by water is available as an option. The maximum stroke frequency is at 90 to 100 cycles per minute for 50% duty cycle. Suction pressures lower than the indicated "pA min" are not permitted and can cause dammages on the unit.



## Redox Flow Battery: Gildemeister, FB 200-400

	FB 200-400	FB 200-800	FB 200-1600
Power and energy			
Rated charge/discharge power* AC		200 / 200 kW	
Energy capacity	400 kWh	800 kWh	1600 kWh
Energy efficiency storage system (AC)		up to 65%	1
Energy efficiency on cell level (DC)		up to 85%	
Charge level		0 100%	
Typ. number of cycles		> 20,000	
AC connections			
Nominal AC voltage		400 V, 3-phase	
Nominal frequency		50 Hz	
Nom. AC current per phase 230 V		290 A	
Power factor (cos φ)		-1 +1	
Reaction time (grid parallel mode)		<3s	
Discharge time at constant power**	1.8 hrs	3.6 hrs	7.1 hrs
140 kW	2.9 hrs	5.8 hrs	11.6 hrs
80 kW	5.5 hrs	11 hrs	22 hrs
Self-discharge			
Self-discharge (shut down mode***)		< 1% per year	
Self-discharge (hot stand-by****)		< 3 kW	
Noise emission			
Sound level (distance 3 m)		< 75 dB(A)	
Mechanical data			
Footprint L x W	6.3 m x 3.6 m	12.6 m x 3.6 m	12.6 m x 7.2 m
	(20.6 ft x 11.8 ft)	(41.3 ft x 11.8 ft)	(41.3 ft x 23.6 ft
Height		5.8 m (19.0 ft)	<u></u>
Weight empty			
Power unit:	13 t (28 660 lbs)	13 t (28 660 lbs)	18 t (39 700 lbs)
Energy unit:	5 t (11 000 lbs)	10 t (22 050 lbs)	20 t (44 050 lbs)
Weight filled with electrolyte			i
Power unit:	14 t (30,900 lbs)	14 t (30,900 lbs)	19 t (41 900 lbs)
Energy unit:	43 t (94,800 lbs)	86 t (189,600 lbs)	172 t (379 200 lbs
Protection rating		IP 54	
Climatic operation conditions			
Ambient temperature	constant ambient te	emperature from -20	to + 40 °C
(storage and operation)	(-4 F to 104 F);	peratare from 20	
Altitude		ft) above sea level	

<sup>\*</sup> all data measured at an electrolyte temperature of 30°C (86 °F)

<sup>\*\*</sup> Approximate discharge time (starting from CL=100%), at continuous stated power. Actual times may vary depending on operating conditions. Remaining energy capacity delivered at derated power.

<sup>\*\*\*</sup> shut down mode: CELLCUBE® is switched off

<sup>\*\*\*\*</sup> hot stand-by: state in which electrolytes are circulating



## **Electrical Charger: EVTec espresso&charge**

AC Ausgang	AC-Steckdose	IEC 62196 Mode	3, Type 2			
Steckdose	Nominale AC Ausgangsleistung	22 kW				
	Nominale AC Ausgangsspannung	400 V <sub>AC</sub>				
	Nominaler AC Ausgangsstrom	3 x 32 A <sub>AC</sub>				
	Sicherheit	<ul><li>Fehlerstromschut:</li><li>Überstromsicheru</li><li>Erdungsüberwach</li></ul>	ng	3)		
DC Ausgänge	DC Stecker	Stecker 1	Stecker 2	Stecker 3		
		CSS IEC 62196-3	CHAdeMO CHAdeMO JEVS G105	Type 2 DC IEC 62196		
	Maximale DC Ausgangsleistung	20 kW - 150 kW				
	DC Ausgangs Spannungwsbereich	170-1000 V <sub>DC</sub> (un	der load: 50-500 \	√ <sub>DC</sub> )		
	Maximaler DC Ausgangsstrom	50 - 300 A <sub>DC</sub>				
	Leistungsfaktor ( > 50% Ladung)	> 0.99				
	Effizienz	93% bei Volllast				
	Sicherheit	<ul><li>Kurzschlussicheru</li><li>Überstromsicheru</li><li>Überspannungsso</li></ul>	ng - Isolations	nnungsschutz überwachung iberwachung		
Allgemein	Betriebstemperatur	-20°C to +45°C				
Augement	Lagertemperatur	-40°C to +85°C				
	relative Luftfeuchtigkeit	5% to 95% (nicht	kondensierend)			
	Schutzklasse	IP54 (Innen-/Ausse	engebrauch)			
	Dimensionen (T x B x H)	930 x 2000 x 850 mm				
	Gewicht	circa 400 kg				
Standards	elektrische Sicherheit (xFC1)	IEC 61851-1, IEC 61439-2				
otariaai ao	EMV	IEC 61851-1, IEC 61439-2 EN 61000-6-1, -2, -3, 4, EN 61000-3-2				
	CHAdeMO	Rev. 0.9.1 (zertifiziert), Rev 1.0.1 (kompatibel)				
	Combined Charging System (CCS)	DIN 70121 (Interopliso 15118		W, VW, GM)		
		Plug IEC 62196-3				

Product: espresso&charge Variant: 3in1, DC Input

Input: 400Vac / 3Ph / 63A / 50Hz
Output: CCS 500Vdc 200A max

CHAdeMO 500Vdc 135A max AC Plug 400Vac 63A max



## DC/DC converter for electrical charger: Brusa, BDC546-B06 (bidirectional)

HIGHSIDE	BDC546-B	UNIT
Min. operating voltage (full performance, highside must not be below lowside)	150	V <sub>DC</sub>
Max. operating voltage (full performance)	750	V <sub>DC</sub>
Overvoltage, the switch-off threshold of the power stage can be set up to	800	V <sub>DC</sub>
Max. voltage, no operation, max. 1 min	900	V <sub>DC</sub>

LOWSIDE	BDC546-B	UNIT
Min. starting voltage	0	V <sub>DC</sub>
Min. operating voltage (full performance)	50	V <sub>DC</sub>
Max. operating voltage (full performance)	600	V <sub>DC</sub>
Overvoltage, switch-off threshold of the power stage (default value)	650	V <sub>DC</sub>
Max. voltage, no operation, max. 1 min	900	V <sub>DC</sub>

POWER DATA	BDC546-B	UNIT
Lowside continuous current (at T <sub>coolant</sub> = 60 °C)	300	Α
Lowside peak current	400	Α
Highside peak current	350	Α
Continuous output power in buck mode (at U <sub>LS</sub> = 600 V)	180	kW
Continuous output power in boost mode (at U <sub>LS</sub> = 600 V)	180	kW
Peak output line	220	kW
Switching frequency	41	kHz

DYNAMIC BEHAVIOUR	BDC546-B	UNIT
Highside voltage step response (in boost mode at $U_{HS}$ = 200 V, $\rightarrow$ 400 V, $I_{LS}$ = 100 A, $U_{LS}$ = 150 V)	< 3	ms
Lowside voltage step response (in buck mode at $U_{LS}$ = 50 V, $\rightarrow$ 300 V, $I_{LS}$ = -200 A, $U_{HS}$ = 500 V)	< 3	ms
Limiting frequency of the superordinate control	1	kHz

STANDBY MODE	BDC546-B	UNIT
Type. Current consumption at AUX (control connector) at $U_{HV}$ = 0 V, $U_{LV}$ = $U_{AUX}$ = 14 V, enable = low	0.731	mA
Type. Current consumption at AUX (control connector) at $U_{HV}$ = 0 V, $U_{LV}$ = $U_{AUX}$ = 14 V, enable = high	247.0	mA

GALVANIC ISOLATION	BDC546-B	UNIT
Voltage resistance between highside/lowside and control circuit (2 s test voltage)	3000	V <sub>DC</sub>

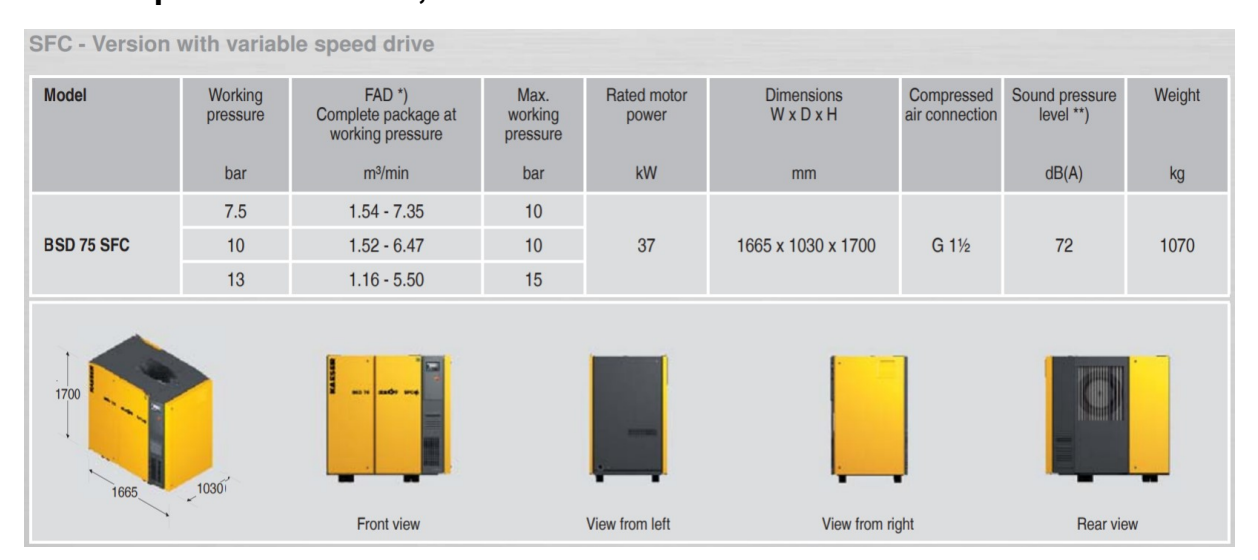


THERMAL / COOLING SYSTEM	BDC546-B	UNIT
Coolant (water / glycol mixing ratio)	50 / 50	
Amount of coolant in device	1100	ml
Min. coolant temperature at the input	-40	°C
Max. coolant temperature at the input	65	°C
Coolant pressure drop at 15 I / min, T <sub>coolant</sub> = 25 °C	< 0.25	bar
Cooling water flow rate max.	17	I/min
Cooling water flow rate min.	15	I/min
Max. cooling system pressure	2.0	bar
Ambient temperature range for storage	-40 to +105	°C
Ambient temperature range in operation	-40 to +85	°C

EFFICIENCY	BDC546-B	UNIT
Efficiency (in buck mode at $U_{HS}$ = 600 V, $U_{LS}$ = 400 V, $I_{LS}$ = 300 A)	98.9	%

BASIC MECHANICAL DATA	BDC546-B	UNIT
Weight (without cooling water)	25.2	kg
Housing material	AlMgSi1	
IP protection	IP6K6 / IP6K7	
Housing volume	14.3	1
Length	640	mm
Width	280	mm
Height	80	mm
External diameter of cooling water connection ports	18.0	mm

## Air compressor: Kaeser, BSD 75 SFC





## List of component suppliers

#### Sensors

- American Sensor Technologies: various pressure sensors, from 200 to 900 bar
- Baumer: level sensor up to 100 bar. Model CleverLevel LBFI
- Carlo Gavazzi: power meter. Model EM200
- Cosmos: Gas detector to detect explosive atmosphere. Model KD-12B
- E+E Elektronik: flow sensor for compressed air. Model EE741-A6D2AC2DN25
- Gems Sensors&Controls: optical level sensor. Model ELS-950
- Gems Sensors&Controls: various pressure sensors, from 10 to 80 bar
- Honeywell: optical level sensor, up to 25 bar. Model LLN865172-1
- Kem Küppers: Coriolis mass flow meter. Model TCMH 0450 SPPS and SRPS
- Michell Instruments: dew point transmitter. Model Easidew
- Valco: continuous level sensor. Model LCT EA52
- Voegtlin: mass flow meter. Model Red-y GSM

#### Control valves

- Bürkert: various solenoid valves for hydrogen production, purification and supply storage
- Bürkert: explosion proof rotary actuator. Model 3004
- Maximator: 2 way straight valve air operated normally close, for hydrogen, 1050 bar

#### **Pumps**

- Edwards: vacuum pump. Model nXDS 15i
- Grundfos: centrifugal pump. Model CM1
- Grundfos: circulator pump. Model Alpha 2 d
- Sawa pumpen: peripheral pump with magnet coupling. Model MP68 -RKME
- Verder: rotary gear pump. Model VG50

#### **Others**

- Alfalaval: various brazed plate heat exchangers
- Classic filters: PTFE filter housing and filter elements for liquids. Model SS424
- Huber: water chiller. Model Unichiller 055T



- Maximator: various high pressure tubing (1/4) and fittings
- Siemens: various electronic components for control systems
- Stäubli: fueling nozzle for 35 MPa hydrogen. Model CHV08
- Swagelock: cylinders for the pressure swing system and various high pressure fittings
- WEH: fueling nozzle for 70 MPa hydrogen. Model TK17 H2

## **Open Access publications**

#### **World Electric Vehicle Journal**

World Electr. Veh. J. 2018, 9(1), 3; <a href="https://doi.org/10.3390/wevj9010003">https://doi.org/10.3390/wevj9010003</a>

#### **Batteries**

Batteries 2018, 4(4), 54; <a href="https://doi.org/10.3390/batteries4040054">https://doi.org/10.3390/batteries4040054</a>

## Liste des abréviations

BEV Battery Electric Vehicle

BMS Battery Management System

CREM Centre de Recherches Energétiques et Municipales

EMPA Swiss Federal Laboratories for Materials Science and Technology

ESS Energy Storage System

FCEV Fuel Cell Electric Vehicle

HRS Hydrogen Refilling Station

LEPA Laboratory of Physical and Analytical Electrochemistry

MV Medium Voltage

PEM Proton exchange membrane
PLC Programmable Logic Controller
VRFB Vanadium Redox Flow Battery

SCCER Swiss Competence Center for Energy Research

SFOE Swiss Federal Office of Energy

